의학 박사학위논문

Cytotoxic effects of escin on human castration-resistant prostate cancer cells through the induction of apoptosis and G2/M cell cycle arrest

인체 호르몬불응성 전립선암 세포주에서 Escin 의 세포고사 및 세포주기 억제 기전에 관한 연구

2014년 8월

서울대학교 대학원

의학과 비뇨기과

PIAO SONGZHE

의학 박사학위논문

인체 호르몬불응성 전립선암 세포주에서 Escin 의 세포고사 및 세포주기 억제 기전에 관한 연구

지도교수 김현회

이 논문을 의학박사 학위논문으로 제출함

2014년 4월

서울대학교 대학원

의학과 비뇨기과 전공

PIAO SONGZHE

PIAO SONGZHE 의 박사학위논문을 인준함

2014년 6월

위 원 장 _____ (인)

부 위 원 장_____(인)

위 원 _____(인)

위 원 _____(인)

위 원 _____(인)

Cytotoxic effects of escin on human castration-resistant prostate cancer cells through the induction of apoptosis and G2/M cell cycle arrest

by

PIAO SONGZHE

A Thesis Submitted to the Department of Medicine in Partial Fulfillment of the Requirements for the

Degree of Doctor of Philosophy in Medicine Science (Urology) at Seoul National University College of Medicine

June 2014

Approved by Thesis Committee:

Professor _____Chairman

Professor _____Vice chairman

Professor _____

Professor _____

Professor _____

Abstract

Cytotoxic effects of escin on human castration-resistant prostate cancer cells through the induction of apoptosis and G2/M cell cycle arrest

PIAO SONGZHE

Department of Urology

The Graduates School

Seoul National University College of Medicine

The progression of prostate cancer to the lethal castration-resistant stage coincides with the high mortality and poor outcome due to loss of successful treatment options and requires the discovery of more potent agents. Escin is known to have cytotoxic

effects on several tumor types, but little is known in the context of prostate cancer. The aim of the present study was to investigate the effects of escin on human castration- resistant prostate cancer (CRPC) cells, PC-3 and DU-145, both *in vitro* and *in vivo*.

The inhibition of cell proliferation and its mechanism were assessed through a cytotoxicity assay, flow cytometry, and a western blot. The *in vivo* efficacy of escin in PC-3 and DU-145 cells was assessed using a xenograft tumor model subcutaneously established in BALB/c nude mice.

The treatment with escin significantly reduced cell viability of PC-3 and DU-145 cells in a dose- and time-dependent manner. In both PC-3 and DU-145 cells, treatment with escin induced apoptosis in a time-dependent manner, which was accompanied by increases in pro-apoptotic (Bax, cleaved-caspase3, and cleaved-PARP) proteins and decreases in anti-apoptotic (XIAP, cIAP-1, cIAP-2, Bcl-2, and Bcl-xL) proteins. In both PC-3 and DU-145 cells, escin treatment caused G2/M-phase cell cycle arrest and thus led to a significant decrease in the expression of cyclin B1 and its activating partner CDK1, with the concomitant induction of $p21^{WAF1/CIP1}$. In addition, escin significantly inhibited the growth of PC-3 and DU-145 cells xenografts subcutaneously established in BALB/c nude mice

In sum, this study provides evidence that escin not only induced cytotoxic effects on PC-3 and DU-145 cells through the induction of apoptosis and G2/M cell cycle

arrest, but also suppressed tumor growth in xenograft models, in support of its efficacious potential as a novel therapeutic agent for CRPC.

……

Keywords: Escin; Castration-Resistant Prostate Cancer; Apoptosis; Cell Cycle

Student Number: 2012-30777

Contents

List of Tables

List of Figures

Introduction

Prostate cancer is the most common cancer in males and a leading cause of cancer mortality in the U.S (Baade, Youlden et al. 2009, Siegel, Ma et al. 2014). The incidence of prostate cancer is quickly rising in Korea (Jung, Won et al. 2014). In 2014, prostate cancer is estimated to be responsible for 233,000 new cases, with 29,480 deaths in the United States alone (Siegel, Ma et al. 2014). In Korea, the number is 13,650 and 1,706, respectively (Figure 1) (Jung, Won et al. 2014). In the early stage, localized prostate cancer can be treated and is potentially curable when detected early. Surgery and androgen-depletion therapy can improve the survival rate of patients. A variety of therapy modalities are effective including radical prostatectomy, hormone therapy, chemotherapy, radiation therapy, and cryotherapy. Unfortunately, despite recent advances in detection and localized curative treatment, after a few years of androgen ablation therapy the disease is likely to recur and become androgen independent. About 23% to 40% of those patients go on to develop metastatic disease (Nadiminty, Tummala et al. 2012) (Figure 2 and 3). Commonly, metastatic disease is treated with androgen-deprivation therapy to induce apoptosis of tumor cells or arrest growth (Kao, Martiniez et al. 2014). However, a lack of successful treatment options for castration-resistant prostate cancer (CRPC) remains a serious problem reflecting a high mortality rate (Kirby, Hirst et al. 2011). Therefore, it is imperative to identify new and effective therapeutic drugs for CRPC.

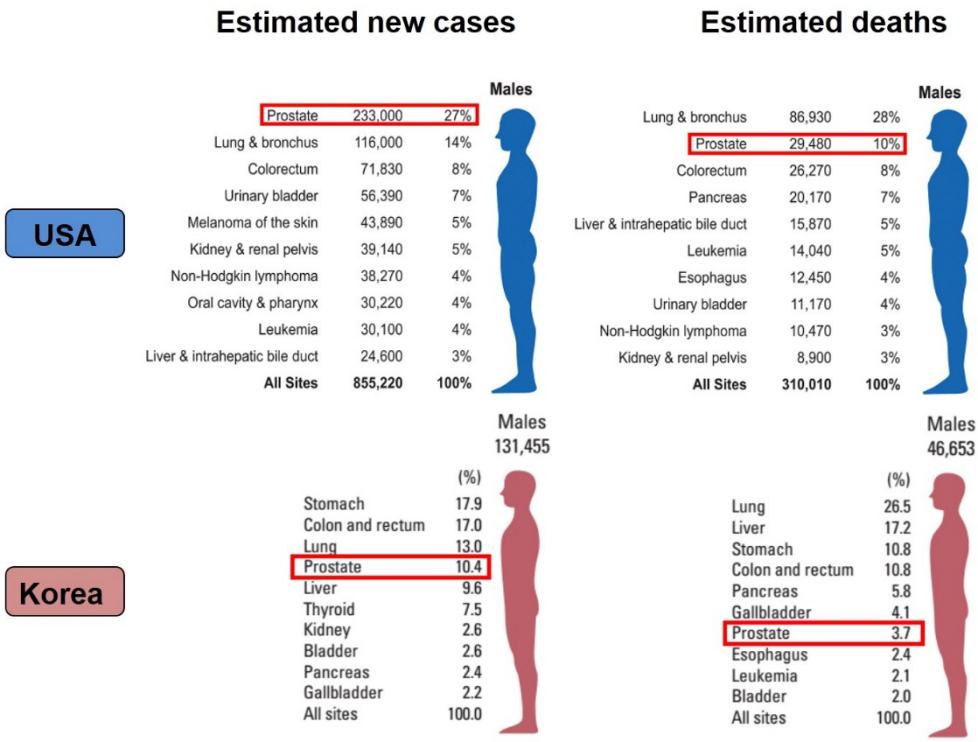

Figure 1. Ten leading cancer types for the estimated new cancer cases and deaths by sex in the United States and Korea in 2014. (Jung, Won et al. 2014, Siegel, Ma et al. 2014)

Prostate cancer is the most frequently diagnosed cancer in males and a leading cause of cancer mortality in the United States. In Korea, prostate cancer is the fourth most common cancer and the seventh leading cause of cancer mortality.

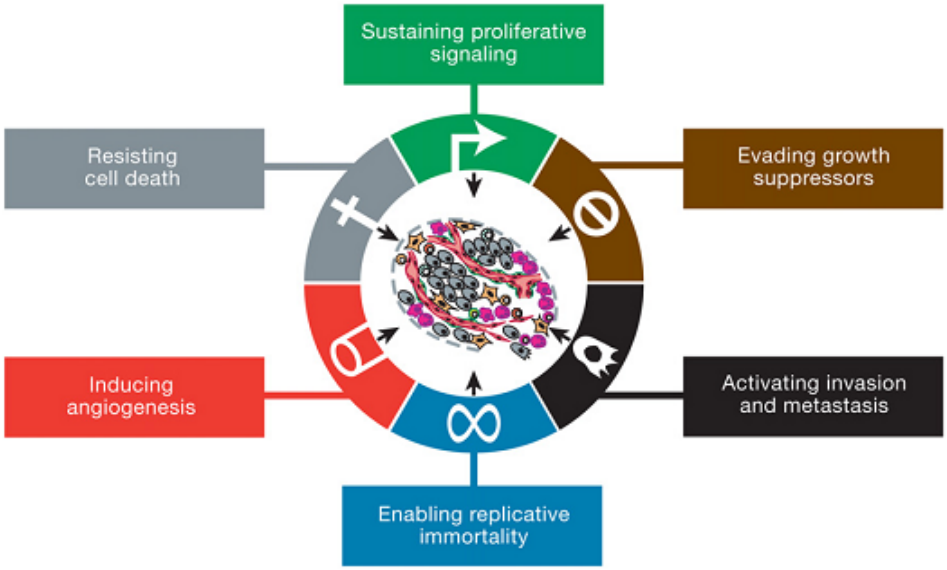

Figure 2. The hallmarks of cancer (Hanahan and Weinberg 2000)

The six hallmarks of cancer—distinctive and complementary capabilities that enable tumor growth and metastatic dissemination continue to provide a solid foundation for understanding the biology of cancer.

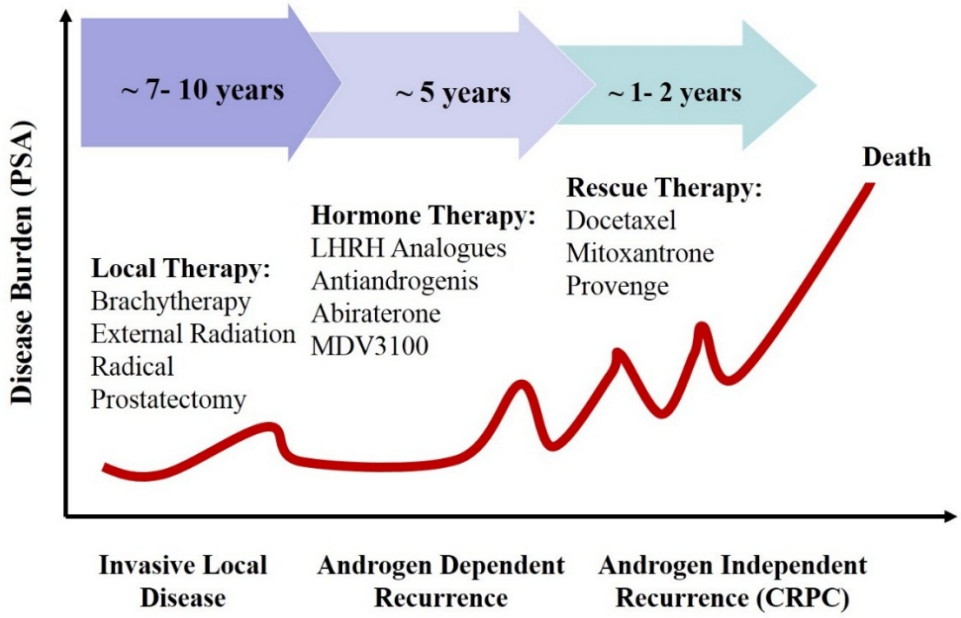

Figure 3. Typical recurrent prostate cancer outcome

When prostate cancer is first diagnosed, it is treated locally by surgery or radiation, and this therapy is often completely successful. However, in about a third of patients, disease recurs. First-line therapy for recurrent prostate cancer is focused on depriving the cancerous prostate cells of access to activated androgen receptor. But eventually this approach becomes ineffective, as almost all patients eventually develop CRPC, which no longer responds to either androgen suppression or blocking of the ligand-binding domain of the androgen receptor. At the symptomatic CRPC stage, treatment options focus on cytotoxic agents such as Docetaxel, and on a newly-approved immunotherapeutic agent, Provenge. Both treatments extend life by an average of four months. Unfortunately, when those second-line therapies fail, patients will typically die within a few months.

Apoptosis is an ordered and orchestrated cellular process that occurs in physiological and pathological conditions. In some, the problem is due to too much apoptosis, such as in the case of degenerative diseases while in others, too little apoptosis is the culprit. Cancer is one of the scenarios where too little apoptosis occurs, resulting in malignant cells that will not die. The mechanism of apoptosis is complex and involves many pathways. Apoptosis is characterized by progressive cell shrinkage (early event) with condensation and fragmentation of nuclear chromatin (late event) (Huerta, Goulet et al. 2007). Caspases are central to the mechanism of apoptosis as they are both the initiators and executioners. There are three pathways by which caspases can be activated. The two commonly described initiation pathways are the intrinsic (or mitochondrial) and extrinsic (or death receptor) pathways of apoptosis (Figure 4). Both pathways eventually lead to a common pathway or the execution phase of apoptosis. A third less well-known initiation pathway is the intrinsic endoplasmic reticulum pathway (O'Brien and Kirby 2008). Apoptosis plays an important role in the treatment of cancer as it is a popular target of many treatment strategies.

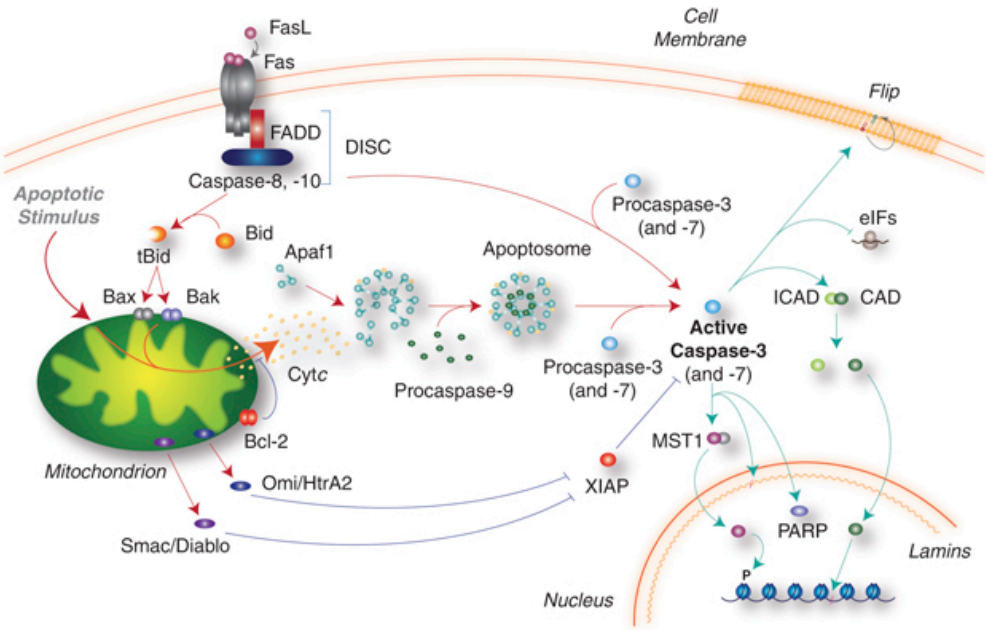
FasL
Fas
Cell
Membrane
Flip
FADD
DISC
Caspase-8, -10
Apoptotic
Stimulus
Procaspase-3
(and -7)
eIFs
tBid
Bid
Apaf1
Apoptosome
ICAD
CAD
Bax
Bak
Active
Caspase-3
(and -7)
Cytc
Procaspase-9
Procaspase-3
(and -7)
MST1
Bcl-2
Mitochondrion
Omi/HtrA2
XIAP
Smac/Diablo
PARP
Lamins
P
Nucleus

Figure 4. Intrinsic and extrinsic pathways of caspase activation in mammals (D'amelio, Cavallucci et al. 2009)

Activation of executioner caspases-3 and -7 is the key event in mammalian apoptosis,. The intrinsic pathway involves the mitochondrion, which acts as an intracellular death receptor receiving a variety of proapoptotic signals that trigger oligomerization of proapoptotic proteins (Bcl-2-associated protein, Bax, and Bcl-2-antagonist killer, Bak, to produce mitochondrial outer membrane permeabilization). This leads to the release of cytochrome c, which activates Apaf1, induction of apoptosome formation, procaspase-9 recruitment/activation and direct processing and activation of procaspase-3 and -7. In the extrinsic pathway, Fas receptor ligand (FasL) triggers the membrane-bound Death-Inducing Signaling Complex (DISC), which recruits procasapase-8 and activates caspase-3 directly. The activation of caspase-3 and -7 is antagonized by IAPs, which in turn can be inhibited by Smac/Diablo and Omi/HtrA2. Activation of caspase-3 and -7 orchestrates the demolition of the cell by cleavage of specific substrates, such as ICAD, Rho effector ROCK1, kinase MST1,PARP, transcription and translation initiation factors.

Cell cycle involves four sequential phases that go from quiescence (G0 phase) to proliferation (G1, S, G2, and M phases) and back to quiescence (Figure 5) (Norbury and Nurse 1992). Progression through the mammalian cell cycle requires the accurate orchestration of a sequence of events. Among the countless elements taking part in this process, the sequential activation of heterodimeric CDK–cyclin complexes (cyclins and their counterpart cyclin-dependent kinases (CDKs)) has been described as the key regulatory events (Shapiro 2006, Malumbres and Barbacid 2007). In addition, there are a number of CDK inhibitors (p21) and a number of other molecules that either regulate or carry out the downstream events, such as the pocket proteins (Rb, p107, p130), the E2F family of transcription factors and the mitosis components (Table 1).

Acquired resistance towards most endogenous apoptosis signaling mechanisms and deregulation of cell cycle checkpoints are believed to promote aberrant proliferation of cancer cells (Gottesman 2002). Defects can occur at any point along these pathways, leading to malignant transformation of the affected cells, tumor metastasis and resistance to anticancer drugs. Any compound aimed at controlling these processes would be beneficial in suppressing the progression of tumors.

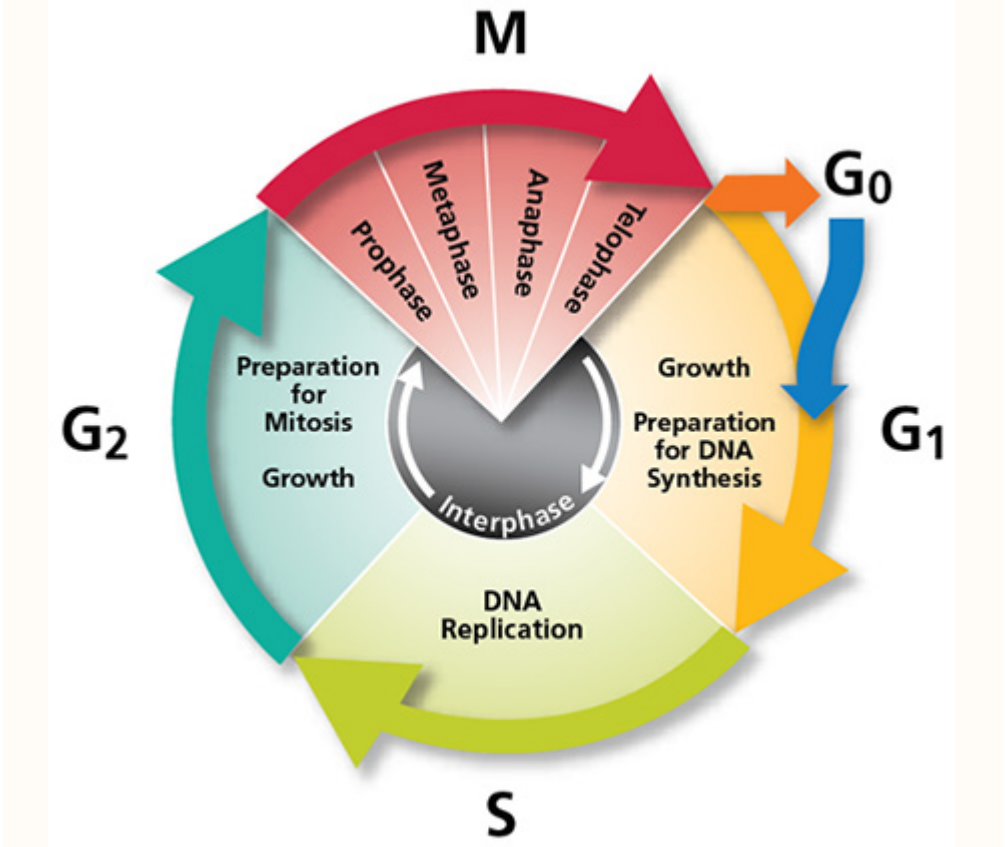

Figure 5. Cell cycle phases

cell cycle in terms of four stages: G_1, when a cell grows and carries out its regular cellular functions; S, when the cell replicates its DNA, resulting in duplicated chromosomes; G2, when a cell continues to grow and prepares itself for cell division; and M, the phase where the cell divides itself into two genetically identical daughter cells. The M phase involves both a nuclear division (called mitosis) and a cytoplasmic division (called cytokinesis).

Table 1. Molecular components of the cell cycle signaling system (Berridge 2007).

Cell cycle component	Comments
Cyclins	Associates with CDK2
Cyclin A1	Associates with CDK2
Cyclin A2	Associates with CDK1
Cyclin B1	Associates with CDK1
Cyclin D1	Widely expressed, interacts with CDK4 and CDK6
Cyclin D2	
Cyclin D3	
Cyclin E1	Associates with CDK2
Cyclin E2	Associates with CDK2
Cyclin H	Associates with CDK7 to form the cyclin- dependent kinase (CDK)- activating kinase (CAK)
Cyclin/ CDK-associated proteins	
Mat1	Stabilizes the cyclin H/ CDK7 complex that form the CAK
Cyclin-dependent kinases (CDKs)	
CDK1	
CDK2	
CDK4	
CDK6	
CDK7	A component of the CAK
CDK inhibitors	
Cip/ Kip family	
P21	Expression strongly increased by p53
P27	
P57	
P16 family	
$P16^{INK4a}$	Shares the same gene locus as the tumor suppressor alternative reading frame (ARF)
$P15^{INK4b}$	Expression increased by transforming growth factor β (TGF- β)
$P18^{INK4c}$	
$P19^{INK4d}$	
Pocket proteins	
Rb/ p105	
P107	

P130/ Rb12	
E2F family of transcription factors	
E2F1	E2 promotor- binding factor 1
E2F2	
E2F3	
E2F4	
E2F5	
E2F6	
E2F7	
E2F- binding partners	
DP1	
DP2	
Regulatory kinases	
PIKs	
PIK1	Plays a major role in regulating mitosis
PIK2	
PIK3	
PIK4	
Wee1	Phosphorylates Tyr-15 on CDK1
Myt 1	Phosphorylates Thr-14 and Tyr-15 on CDK1
Nek2	A kinase that may plays a priming role in phosphorylating PIk substrates
Citron kinase	Phosphorylates myosin light chain (MLC) during cytokinesis
Checkpoint kinase	
ATM	Ataxia telangiectasia mutated
ATR	ATM- and Rad3- related
Chk1	Checkpoint kinase 1
Chk2	Checkpoint kinase 2
Aurora B	Phosphorylates MgRac- GAP and MYPT1 during cytokinesis
Regulatory phosphatases	
Cdc25	
Cdc25A	Dephosphorylates CDK2 in late G1
Cdc25B	Dephosphorylates CDK1 in late G2/M
Cdc25C	Dephosphorylates CDK1 in late G2/M
Cdc14a	Dephosphorylates components of the spindle midzone complex during cytokinesis

Katanin	A microtubule- severing protein
TRTP	A microtubule- severing protein
Stathmin	A microtubule- destabilizing protein
ASPM	Abnormal spindle protein- like, microcephaly-associated
Chromosome separation	
Cohesin	A protein that “glues” chromatids together during spindle assembly
Securin	A scaffolding protein that inactivates separase
Separase	A cysteine protease that cleaves cohesion
Spindle midzone complex	
MKLP1	Mitotic kinesin- like protein 1
MKLP2	Mitotic kinesin- like protein 2
Plk1	Translocates MKLP2 to the spindle
MgRac-GAP	A Rho- GEF
ECT2	A microtubule- associated protein (MAP)
PRC1	Protein regulator of cytokines 1
KIF1	A kinesin- 4 family member that interacts with PRC1
INCENP	Inner centromere protein
Survivin	Cytokinesis

Escin (or aescin) is the major active principle from Aesculus hippocastanum (Hippocastanaceae) the horse chestnut tree, a plant widely distributed all over the world because of its excellent resistance to environmental conditions. The horse chestnut grows in Iran, Northern India, Asia Minor, South-East Europe, America, from the Balkans to the Caucasus, as well as in the Korea (Fournier 1948). Escin is a natural mixture of triterpene saponins (Figure 6) (Costantini 1999) which exists in two forms, α and β, that can be distinguished by: melting point, specific rotation, haemolytic index and solubility in water. β-escin appears to be the active component of the mixture and is the molecular form present in major available pharmaceutical products. The pharmacological profile of β-escin has received significant contributions in recent years, in order to establish the pharmacological basis for the major clinical indication of treatment of chronic venous insufficiency (CVI) (Pittler and Ernst 2006). Recently, escin has attracted considerable attention because of its anticancer activity. Although many studies have reported that escin shows cytotoxic activity against several cancer cells by inhibiting cell growth and inducing apoptosis and cell cycle arrest (Patlolla, Raju et al. 2006, Harikumar, Sung et al. 2010, Tan, Li et al. 2010, Zhang, Gao et al. 2011), no study has addressed these functions in human prostate cancer cells.

Objective of this study

To evaluate the in vitro and in vivo effects of escin on human CRPC cells, PC-3 and DU-145.

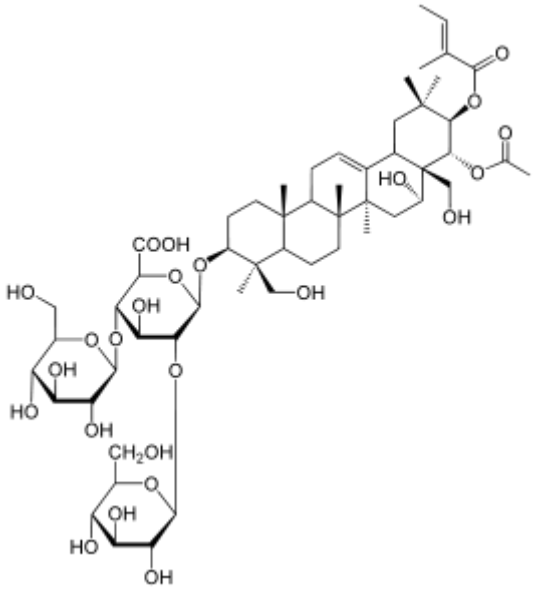

Figure 6. Chemical structure of escin (Fu, Hou et al. 2005)

The main active compound of the extract of Aesculus hippocastanum (the horse chestnut) seeds is escin (C_{54}-H_{84}-O_{23}), a penta cyclic triterpene.

Material and Methods

Cell viability assay

Human PC-3, DU-145, and PNT-2 cells (ATCC™) were cultured in RPMI-1640 medium (Grand Island, NY, USA) supplemented with 10% fetal bovine serum (FBS; Grand Island, NY, USA) in a humidified 5% CO2 atmosphere at 37℃. A 100 mM solution of escin (Sigma-Aldrich, Sigma-Aldrich, St. Louis, MO, USA) was dissolved in dimethyl sulfoxide (Sigma-Aldrich) and diluted as needed in the cell culture medium. To assess the cell viability of PC-3, DU-145 and PNT-2 cells after escin treatment, we used the Cell Counting Kit-8 (Sigma-Aldrich) with escin on relevant cells, 10μl CCK-8 solution was added to 200μl medium in each well. Plates were incubated at 37℃ for 4 hours and shaken on a rotary platform at room temperature (RT) for 10 minutes. Absorbance at 450 nm was measured using a microplate reader. The 24μM dose was selected for further studies based on our preliminary experiments.

Apoptosis analysis

The MBL MEBCYTO Apoptosis Kit (Medical & Biological Laboratories Co., Nagoya, Japan) was used to detect apoptosis. After incubation with 24μM of escin for 6 or 12 hours, PC-3 and DU-145 cells were trypsinized and resuspended in 300μl of binding buffer, and 5μl of Annexin V-FITC and 2.5μl of propidium iodine (PI)

were added to the 300μl of cell suspension. The samples were kept in the dark for 15 minutes and analyzed using a FACSCalibur™ flow cytometer (Becton Dickinson, Heidelberg, Germany).

Cell cycle analysis

PC-3 and DU-145 cells were seeded in 20 mm^2 dishes and cultured with indicate concentrations of escin for 6 or 12 hours. Following incubation, the cells were collected and fixed with 70% ethanol. Samples were treated with 5μl of RNase A (10μg/mL) for 1 hour at 37℃, stained with 10μl of PI (10μg/mL) for 0.5 hour at 4℃, and analyzed with the FACSCalibur™ flow cytometer. Cell cycle distribution (G0/G1, S, and G2/M) was determined from only surviving cells.

Western blotting

After PC-3 and DU-145 cells were treated with 24μM of escin for the indicated time periods, the cells were lysed and total protein concentration was quantified by Bradford reagent (Bio-Rad, Hercules, CA, USA). Equal amounts of protein lysates were separated by sodium dodecyl sulfate-polyacrylamide gel electrophoresis (SDS–PAGE), and transferred to polyvinylidene difluoride (PVDF) membrane (Millipore, Bedford, MA, USA). Interested proteins were probed by primary antibodies and corresponding peroxidase-labeled secondary antibodies followed with detection by

enhanced chemiluminescence (ECL; Millipore Corporation, Billerica, MA, USA). All primary antibodies used in this study are listed in Table 2.

Table 2. List of antibodies used in this study

Antibody	**Source**
cleaved-caspase3 (c-caspase3)	Cell Signaling Techenology
PARP	Cell Signaling Techenology
BCL-2	Cell Signaling Techenology
BCL-xL	Cell Signaling Techenology
BAX	Cell Signaling Techenology
c-IAP1	Cell Signaling Techenology
c-IAP2	Cell Signaling Techenology
xIAP	Cell Signaling
CDK1	EMD Millipore Corporation
p-CDK1	EMD Millipore Corporation
cyclin B1	Cell Signaling
$p21^{Waf1/ Cip1}$	Cell Signaling
β-actin	Sigma

In vivo efficacy of escin treatment in human prostate cancer xenograft model

Specific pathogen-free male BALB/c athymic nude mice (age 4-5 weeks) were purchased from Central Lab Animal (Seoul, Korea). They were allowed to acclimatize for 1 week before initiating the experiment. They were maintained in a 12-hour light/ 12-hour dark cycle under pathogen-free conditions and fed with standard diet and water ad libitum. The Institutional Animal Care and Use Committee of Seoul National University Hospital reviewed and approved all procedures C. PC-3 or DU-145 cells (5×10^6) were suspended in 200 μl of PBS and injected subcutaneously into flanks of each animal. Tumor growth was measured twice weekly using a caliper and body weight was measured weekly. The tumor volume was calculated using the formula: volume (mm^3) = (length × $width^2$) × $\pi/6$. After establishment of palpable tumors of 150 - 200 mm^3, requiring approximately 3-4 weeks, the tumor-bearing mice were randomly assigned to 6 groups (N=5 in each group) receiving dosed intraperitoneally once daily for 3 weeks. The experimental groups were defined as group 1: PC-3 cells treated with vehicle (DMSO in 200 μl PBS), group 2: PC-3 cells treated with low-dose of escin (1.4 mg/kg), group 3: PC-3 cells treated with high-dose of escin (2.8 mg/kg), group 4: DU-145 cells treated with vehicle (DMSO in 200 μl PBS), group 5: DU-145 cells treated with low-dose of escin (1.4 mg/kg), and group 6: DU-145 cells treated with high-dose of escin (2.8 mg/kg) respectively. The doses of escin that selected for this experiment was based on

previous studies (Zhou, Fu et al. 2009). When 3 weeks of treatment finished, the mice were sacrificed. The tumors were harvested and the index of anti-tumor activity assessed is the relative tumor inhibition rate (IR, %) and the formula is as follows: IR (%) = (C − T) / C × 100%, where C is the average tumor weight of the model control group, T is the average tumor weight of medicine groups. Organs including lung, heart, liver, kidney, and spleen were harvested and weighted. The organ index was calculated according to the equation: organ index= the organ weight (mg)/ the body weight (g).

Histologic and immunohistochemistric (IHC) analysis

For histological analysis, tumors as well as lung, heart, liver, spleen, heart, lung and kidney were fixed in 10% buffered formalin, embedded in paraffin, sectioned at 5 μm, and stained with hematoxylin and eosin (H&E). Immunohistochemistry of representative tumor sections were performed for the evaluation of Ki-67 (Dako, Glostrup, Denmark), a marker for proliferating cells, as previously described (Jeon, Jeong et al. 2010). The nucleus of positive cells was stained brown as detected under light microscopy. In each slide, ten high-power (×400) fields were randomly selected and the proliferation index was expressed as the percentage of positive cells relative to the number of total cells in a given area. Apoptosis was confirmed by the terminal nucleotidyl transferase-mediated nick end labeling (TUNEL) assays using a detection kit (Chemicon, Temecula, CA, USA) as previously described. The nucleus of

positive cells was stained brown as detected under light microscopy. In each slide, ten high-power (×400) fields were randomly selected and the apoptotic index was expressed as the percentage of apoptotic cells relative to the number of total cells in a given area.

Statistical Analyses

All *in vitro* experiments were performed more than three times, and the data were represented as the mean ± SD. Because of modest sample size, the nonparametric Kruskal–Wallis test was used to analyze all groups, and the Mann–Whitney U-test was used to compare pairs of groups. Differences were considered significant at $p < 0.05$.

RESULTS

Escin Showed Cytotoxic Effect on human CRPC via Apoptotic Cell Death

The cytotoxic effect of escin was investigated using human CRPC cells (PC-3, DU-145) and normal epithelial prostate cells (PNT-2). Escin specifically inhibited prostate cancer cell proliferation in a dose--and time- dependent manner (Figure 4.a and b, respectively), survival of a normal prostate epithelial cell line (PNT-2) was minimally affected by escin even at the concentration (24 μM) that were highly cytotoxic to the prostate cancer cells (Figure 7. A and B). According to results from the CCK-8 assay in which we tested the efficacy of escin on the growth of CRPC cells, we selected the doses of 24 μM of escin to explore the underlying mechanism of escin-induced proliferation inhibition of the cells. After treatment with 24 μM of escin for 0, 6 and 12 h, prostate cancer cells (PC-3 and DU-145). The apoptotic rate of prostate cancer cells increased significantly in a time-dependent manner, as shown in Figure 8. A (a and b). Flow cytometry revealed that the amount of apoptotic cells present after treatment with 24 μM of escin was 15.66 ± 4.48 at 0 h, 69.02 ± 0.89 at 6 h and 84.11 ± 0.52 at 12 h in PC-3 cells (Figure 8 A. (c)), while the amount was 6.96 ± 1.02 at 0 h, 25.92 ± 0.59 at 6 h and 55.18 ± 0.98 at 12 h in DU-145 cells, respectively (Figure 8. A (d)). In PC-3 and DU-145 cells, escin caused a significant increase in both early and late apoptotic populations in a time-dependent manner compared to control (Figure 8. A). Additionally, we examined the expression of

apoptosis related proteins caspase-3 and PARP by western blot analysis. Escin induced activation of caspase-3 and cleaved PARP (c-PARP) in a time-dependent manner compared to the untreated control cultures as shown in Figure 8. B (a and c). Further, we examined the effect of escin on the expression of Bcl-2 and IAP family members, Western blot analysis data showed that escin time-dependently induced the expression of pro-apoptotic Bax protein, whereas those levels of anti-apoptotic Bcl-2 and Bcl-xL were decreased in response to escin treatment. Therefore, the ratio of Bax/Bcl-2 was increased, which may contribute to apoptosis in prostate cancer cells. The levels of IAP family members such as XIAP, cIAP-1 and cIAP-2 were markedly inhibited by escin treatment in a time-dependent manner (Figure 8. B (b and d). Taken together, we can deduce that escin suppresses the proliferation of prostate cancer cells partially relying on its apoptosis-inducing effect.

A

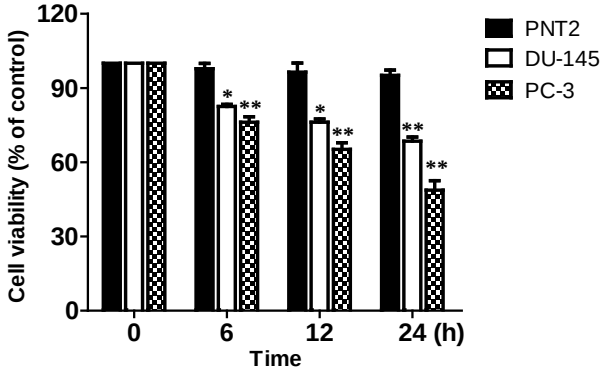

B

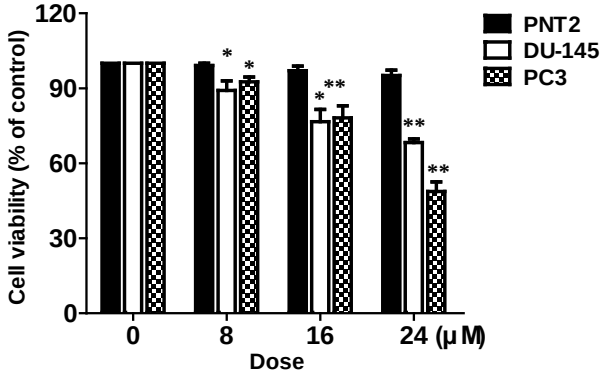

Figure 7. Effect of escin on cell proliferation

Normal epithelial prostate cells (PNT-2) and two types of CRPC cells (PC-3 and DU-145) were grown in the absence or presence of graded concentrations of escin for 6 h, 12 h, and 24 h. The cell proliferation rate was measured using the CCK-8 method. Representative experiments from at least three independent experiments are shown, data are presented as a percentage of the control, and the mean ± SD is given. *, **, and *** indicate significance at the $p<0.05$, $p<0.01$, and $p<0.001$ levels, respectively.

A

a

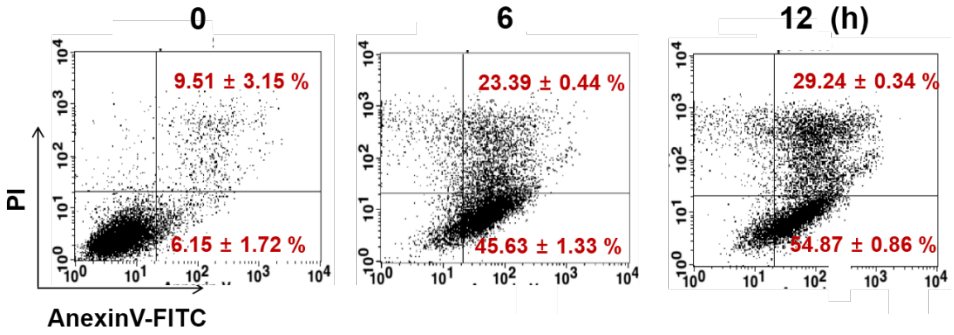
0
6
12 (h)
9.51 ± 3.15 %
23.39 ± 0.44 %
29.24 ± 0.34 %
6.15 ± 1.72 %
45.63 ± 1.33 %
54.87 ± 0.86 %
PI
AnexinV-FITC

b

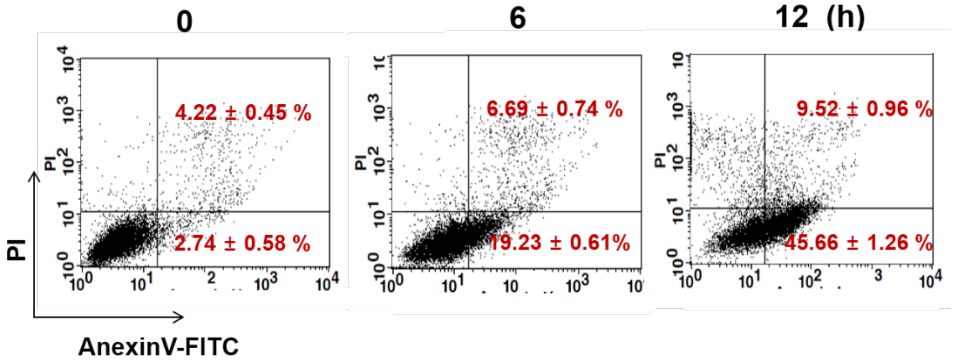
0
6
12 (h)
4.22 ± 0.45 %
6.69 ± 0.74 %
9.52 ± 0.96 %
2.74 ± 0.58 %
19.23 ± 0.61%
45.66 ± 1.26 %
PI
AnexinV-FITC

c

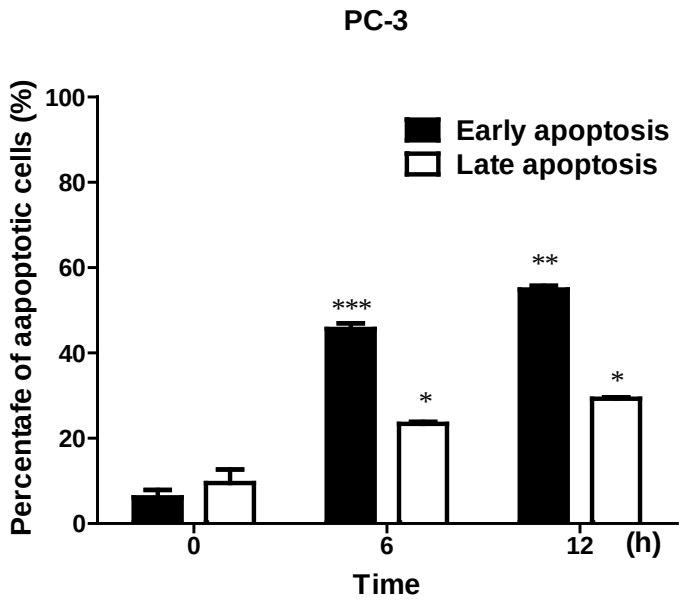
PC-3
Percentafe of aapoptotic cells (%)
100
80
60
40
20
0
Early apoptosis
Late apoptosis
***
*
**
*
0
6
12
(h)
Time

d

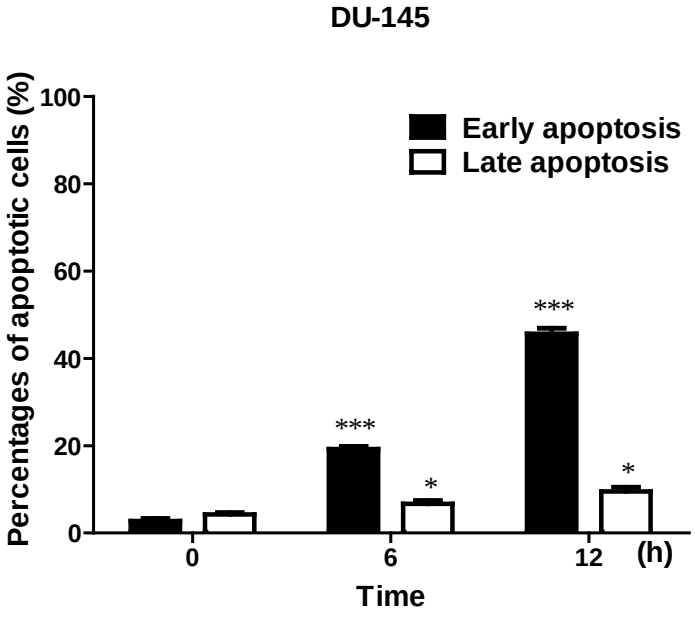
DU-145
Percentages of apoptotic cells (%)
100
80
60
40
20
0
Early apoptosis
Late apoptosis
***
*
***
*
0
6
12
(h)
Time

B

a

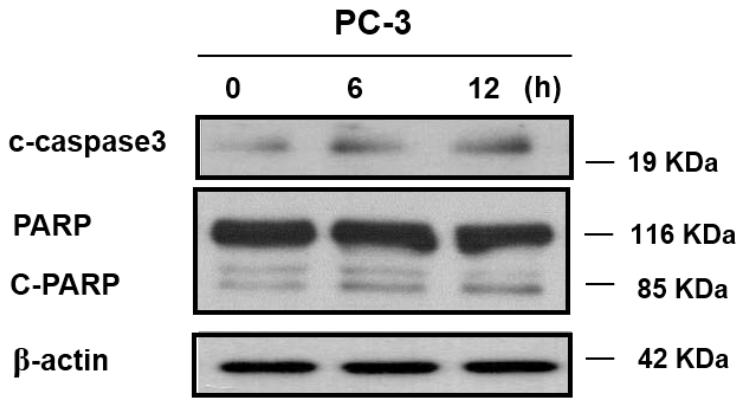
PC-3
0
6
12 (h)
c-caspase3
19 KDa
PARP
116 KDa
C-PARP
85 KDa
β-actin
42 KDa

b

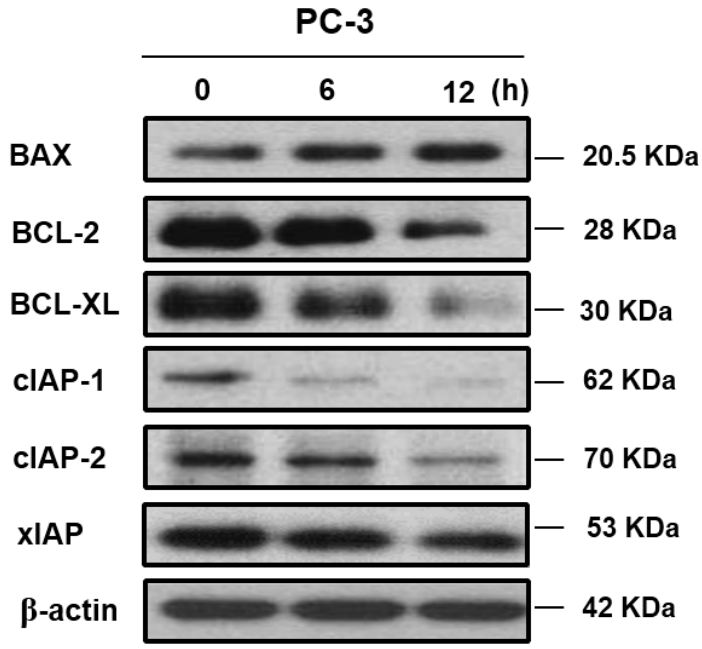
PC-3
0
6
12 (h)
BAX
20.5 KDa
BCL-2
28 KDa
BCL-XL
30 KDa
cIAP-1
62 KDa
cIAP-2
70 KDa
xIAP
53 KDa
β-actin
42 KDa

c

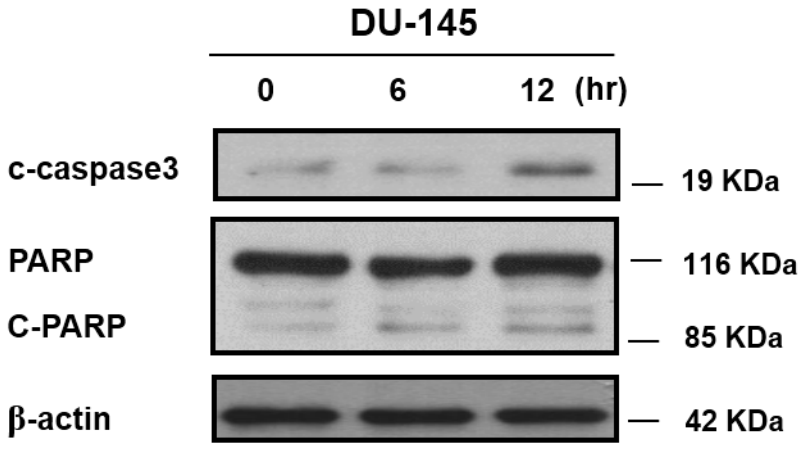
DU-145
0
6
12 (hr)
c-caspase3
19 KDa
PARP
116 KDa
C-PARP
85 KDa
β-actin
42 KDa

d

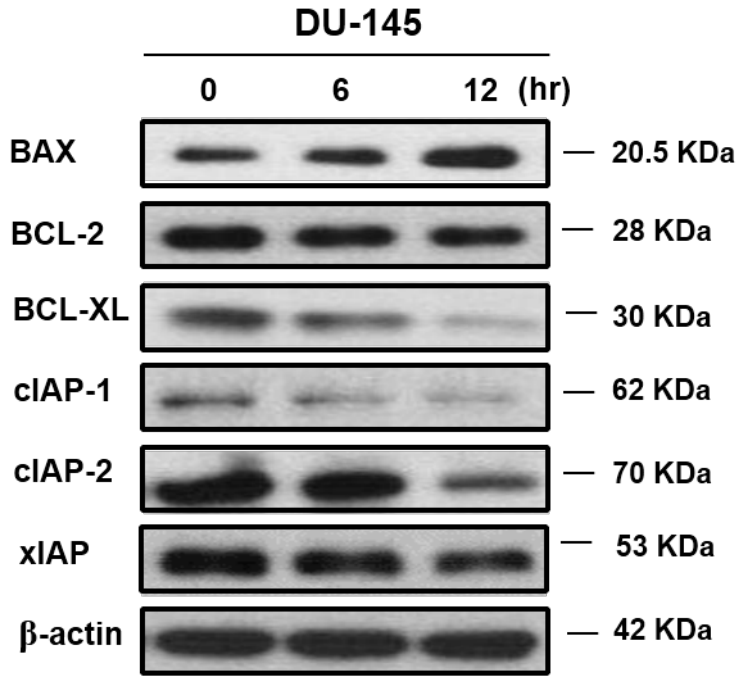
DU-145
0
6
12 (hr)
BAX
20.5 KDa
BCL-2
28 KDa
BCL-XL
30 KDa
cIAP-1
62 KDa
cIAP-2
70 KDa
xIAP
53 KDa
β-actin
42 KDa

Figure 8. Escin suppressed the proliferation of CRPC cells by inducing apoptotic cell death

(A) Flow cytometry data were plotted to compare apoptotic cell populations in each treatment condition. (a) PC-3 cells, (b) DU-145 cells, and (c) quantitative data on (a). (d) Quantitative data on (b). Representative experiments from at least three independent experiments are shown, the mean ± SD is given. *, **, and *** indicate significance at the $p<0.05$, $p<0.01$, and $p<0.001$ levels, respectively. (B) A western blot analysis. C-caspase3, PARP, BcL-2, BcL-xL, Bax, cIAP-1, cIAP-2, xIAP, and c-PARP were detected by a western blot in PC-3 (a and b) and DU-145 (c and d) cells. β-actin was used as a lane loading control.

Escin induces cell cycle arrest at G2/M phase and modulates cell cycle-related gene and protein levels in CRPC cells

In addition to apoptosis, we also tested whether escin could induce cell cycle arrest in CRPC cells. After treatment of PC-3 and DU-145 cells with 24 μM of escin for indicated times (0, 6 and 12 h), we used flow cytometry to detect cell cycle distribution. As shown in Figure 9. A (a and b), treatment of PC-3 and DU-145 cells with escin significantly caused G2/M phase arrest in a time-dependent manner, with a corresponding decrease in the percentage of cells in the G0/G1 and S phase. In PC-3 cells, G2/M phase increased from 12.24 ± 2.46% in the untreated control to 19.72 ± 6.20% and 33.50 ± 1.79%, respectively; G0/G1 phase decreased from 51.35 ± 1.95% to 43.00 ± 0.42% and 41.69 ± 1.14%, respectively, and S phase decreased from 25.73 ± 0.88% to 23.94 ± 1.45% and 18.29 ± 1.61%, respectively, following 6 and 12 h treatment with 24 μM of escin. However, treatment of DU-145 cells with such a low dose of escin for the indicated time didn't significantly change the cell cycle distribution (data was not shown). When the escin concentration was further elevated to 44 μM, the cell population in G2/M phase increased from 12.24 ± 2.46 in the untreated control to 19.72 ± 6.20, and 33.50± 1.79, respectively; G0/G1 phase decreased from 50.00 ± 2.16% to 47.85 ± 2.34% and 45.11± 5.76%, respectively, and S phase decreased from 27.71 ± 2.34% to 26.34 ± 1.83% and 22.56± 1.73%, respectively (Figure 9. A (c and d)). Such observations demonstrate that the threshold for induction of apoptosis was lower than G2/M arrest in DU-145 cells treated with escin. To elucidate the mechanism for G2/M arrest in escin-treated cells, we

determined its effect on expression of genes that are pivotal for G2/M transition, including CDK1 and cyclin B1. After incubation of the cells with escin (24μM in PC-3, 44 μM in DU-145) for 0, 6 and 12 h, respectively, mRNA expression levels were determined using the target gene/ housekeeping gene ratio by setting the control to 100%. Furthermore, we detected the expression level of cell cycle-related proteins such as cyclin B1, CDK1, p-CDK1 and $p21^{WAF1/CIP1}$ to explore the mechanism accounting for G2/M cellcycle arrest. As shown in Figure 9 B, we found that the protein level of cyclin B1 and CDK1 was down-regulated, while the expression level of $p21^{WAF1/CIP1}$ was increased after escin treatment .

A

a

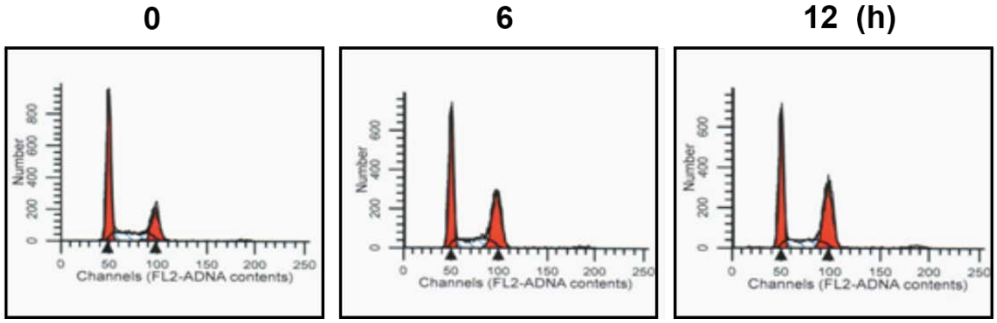
0
6
12 (h)
Number
Channels (FL2-ADNA contents)

b

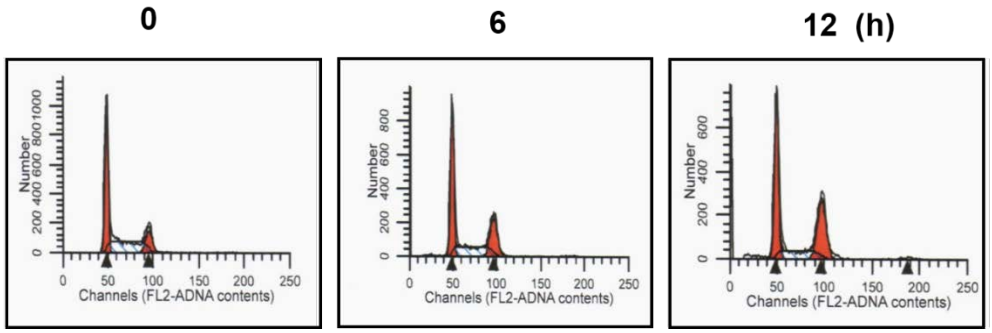
0
6
12 (h)
Number
Channels (FL2-ADNA contents)

c

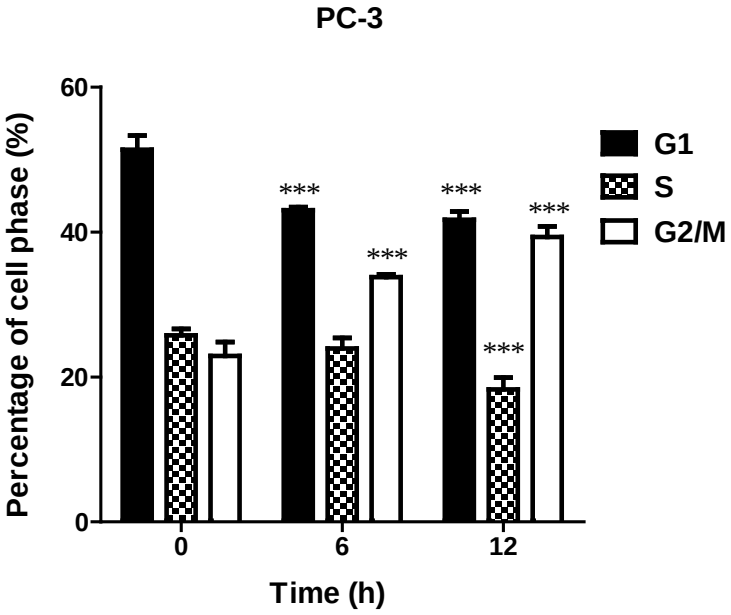
PC-3
Percentage of cell phase (%)
60
40
20
0
***
***
***
***
***
0
6
12
Time (h)
G1
S
G2/M

d

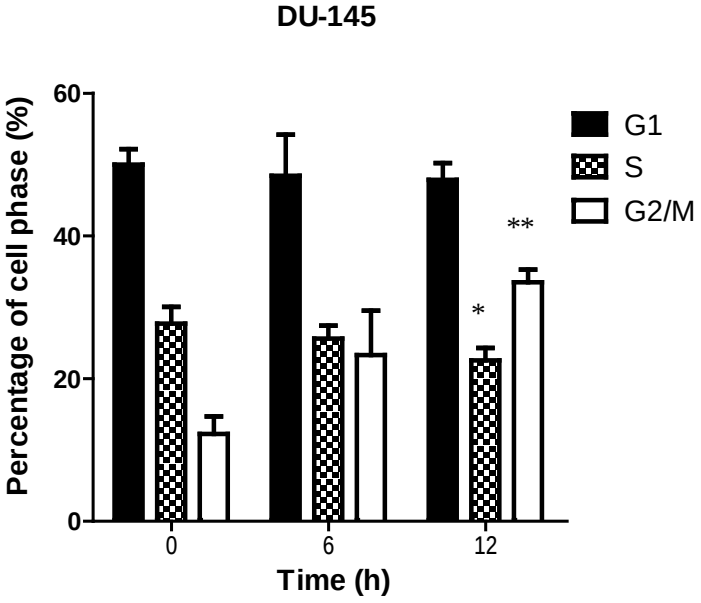
DU-145
Percentage of cell phase (%)
60
40
20
0
*
**
0
6
12
Time (h)
G1
S
G2/M

B

a

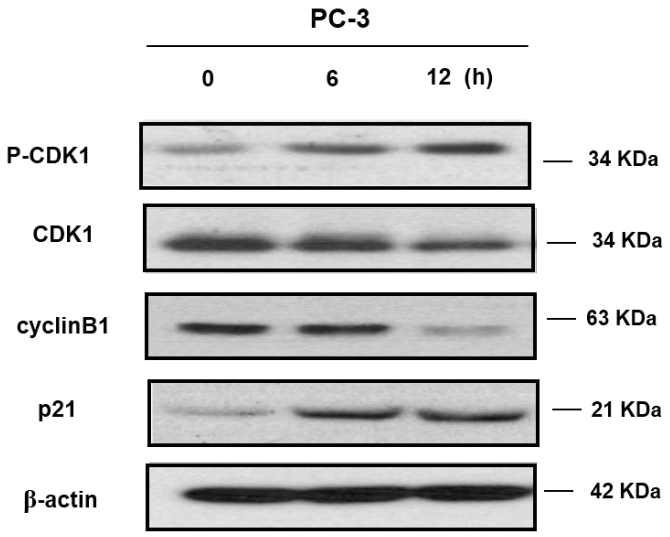
PC-3
0
6
12 (h)
P-CDK1
34 KDa
CDK1
34 KDa
cyclinB1
63 KDa
p21
21 KDa
β-actin
42 KDa

b

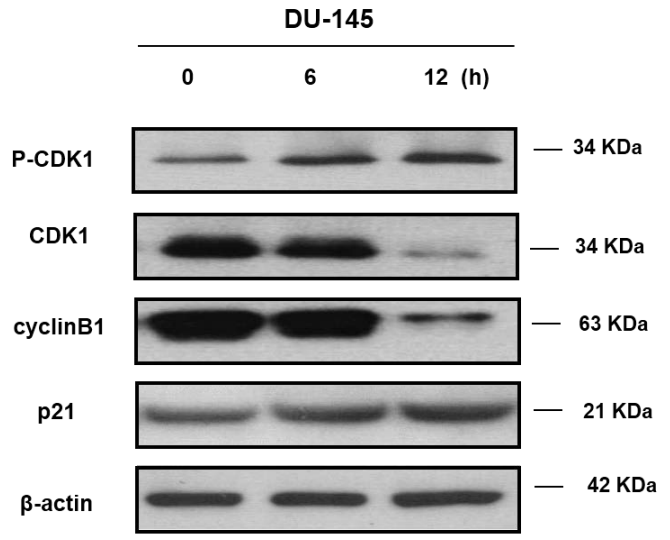
DU-145
0
6
12 (h)
P-CDK1
34 KDa
CDK1
34 KDa
cyclinB1
63 KDa
p21
21 KDa
β-actin
42 KDa

Figure 9. The cell cycle dysregulation induced by escin in human CRPC cells

PC-3 cells were treated with culture medium or 24 μM of escin for indicated times, and DU-145 cells were treated with culture medium or 44 μM of escin for indicated times, respectively. (A) Representative histograms shows the cell cycle distribution of the control and escin-treated (a) PC-3 and (b) DU-145. Percentages of cells present in indicated phases of the cell cycle (G0/G1, S, or G2/M) are shown in (c) PC-3 cells and (d) DU-145. The mean ± SD is given. * and ** indicate significance at the $p < 0.05$ and $p < 0.01$, respectively. (B) Western blot analysis was performed to evaluate the expression of Cyclin B1, CDK1, p-CDK1, and p21 in the escin-treated (a) PC-3 and (b) DU-145. β-actin was used as a lane loading control.

Escin suppresses growth of human prostate cancer in a nude mice xenograft model

Consistent with the anti-proliferative response in vitro with PC-3 and DU-145 cells, escin significantly diminished tumor volume when compared to their respective controls in a dose-pendent manner. Treatment with low dose of escin (1.4 mg/kg) resulted in a significantly decreased mean tumor value in group 2 and group 5, reaching 617.40±120.21 and 715.89 ± 77.54 mm^3, respectively. Treatment with high dose of escin (2.8 mg/kg) also resulted in a significantly decreased mean tumor value in group 3 and group 6, reaching 499.35 ± 54.88 and 600.89 ± 53.47 mm^3. (Figure 10. A and B). Administration of escin significantly decreased the tumor weight (Figure 10. C). The tumor growth inhibition ratio of low dose group and high dose group were 33.53%, 46.07% in PC-3 xenografts, and 13.86% , 28.87% in DU-145 xenografts, respectively (Table 3). We didn't observe dose-related variation in the body weight and the organ index for these treatments (Table 3). Moreover, no discernible injuries could be examined on the H&E stained sections of organs including lung, heart, liver, kidney and spleen (data not shown). This in vivo study confirmed the tumor inhibitory response of escin. To explore the mechanisms of tumor inhibition in vivo, tumors were collected after the animals were sacrificed. First, the tumor sections from control and escin-treated mice were stained with H&E. The staining for H&E was relatively brighter and more intense in tumors of control mice compared with tumors from escin-treated mice (Figure 11. A). These results suggested a relatively higher proliferation index in control tumors than in the tumors

from escin treated mice. We confirmed this speculation by analysis of Ki-67 expression, a well-known proliferation marker. The brown color Ki-67 staining was relatively more intense in control tumors compared with the tumors from escin treated mice (Figure 11. B). These results indicated that escin administration inhibited PC-3 and DU-145 cells proliferation in vivo. To test whether escin-mediated inhibition of PC-3 xenograft growth in vivo was due to increased apoptosis, tumor tissues from control and escin-treated mice were examined for histologic evidence of apoptosis. The apoptotic bodies in tumor sections of control and escin-treated mice were visualized by TUNEL staining and representative micrographs are shown in Figure 11. C. The tumors from escin-treated mice exhibited a markedly higher count of apoptotic bodies compared with control tumors.

A

a

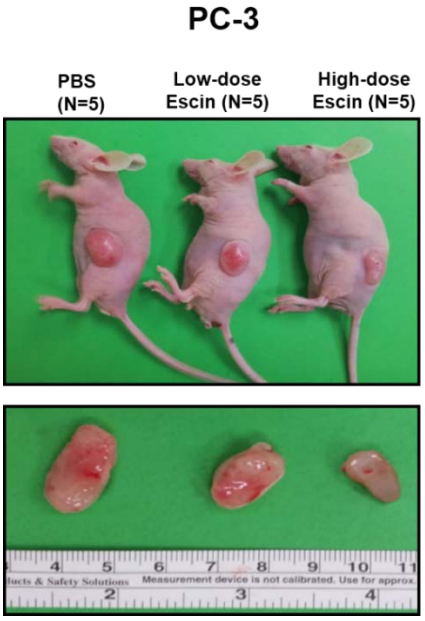
PC-3
PBS (N=5)
Low-dose Escin (N=5)
High-dose Escin (N=5)
Measurement device is not calibrated. Use for approx.

b


DU-145
PBS (N=5)
Low-dose Escin (N=5)
High-dose Escin (N=5)
OR Products & Safety Solutions

B

a

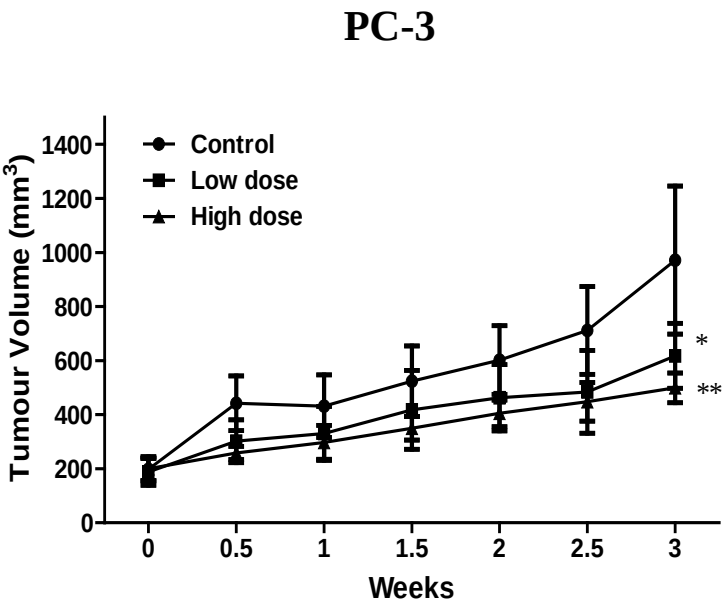
PC-3
Control
Low dose
High dose
Tumour Volume (mm3)
1400
1200
1000
800
600
400
200
0
0
0.5
1
1.5
2
2.5
3
Weeks
*
**

b

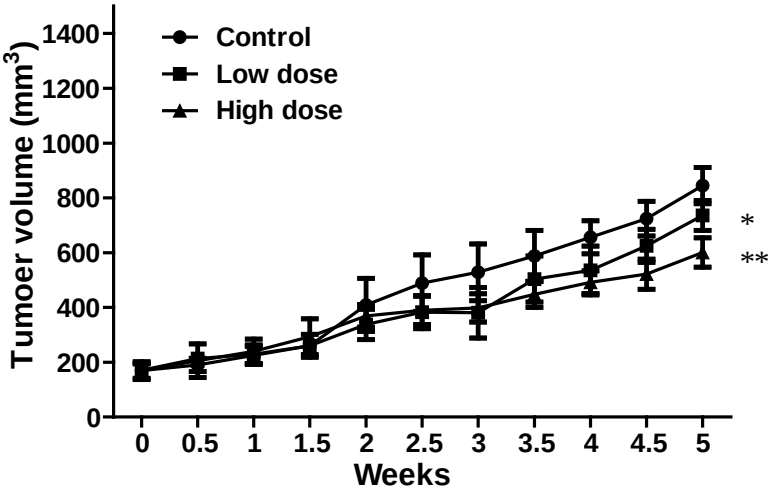
DU-145
Control
Low dose
High dose
Tumoer volume (mm3)
1400
1200
1000
800
600
400
200
0
0
0.5
1
1.5
2
2.5
3
3.5
4
4.5
5
Weeks
*
**

C

a

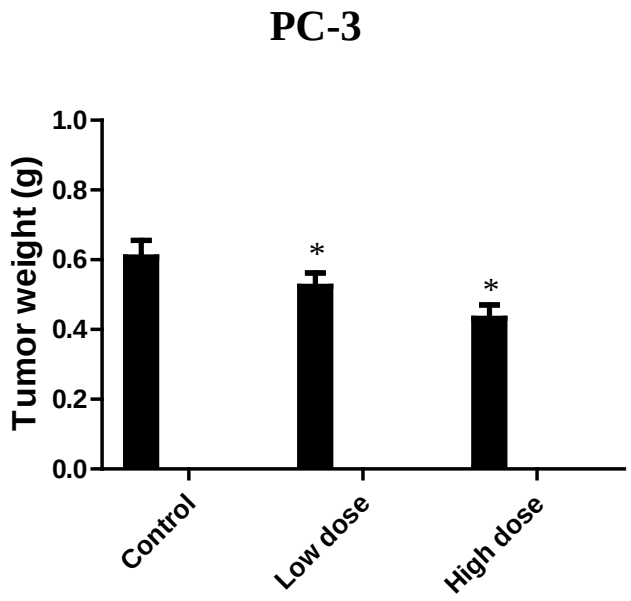
PC-3
Tumor weight (g)
1.0
0.8
0.6
0.4
0.2
0.0
*
*
Control
Low dose
High dose

b

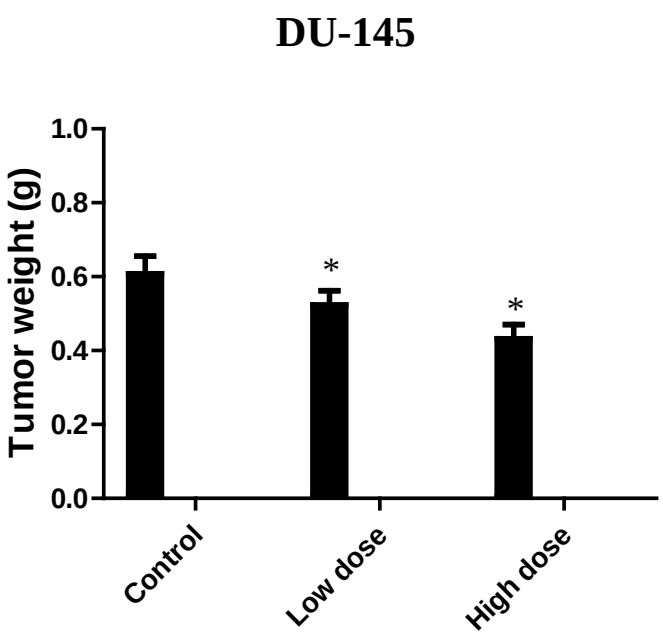
DU-145
Tumor weight (g)
1.0
0.8
0.6
0.4
0.2
0.0
*
*
Control
Low dose
High dose

Figure 10. Reduction of tumor growth by escin treatment in human CRPC xenograft models

(A) Photograph represents the xenografted tumors of (a) PC-3 and (b) DU-145 in the subcutaneous region of nude mice, which excised at the end of the study. (B) Tumor growth curves are shown for the xenografted tumors of (a) PC-3 and (b) DU-145 in the subcutaneous region of nude mice. The average tumor volume in vehicle-treated control mice and mice treated with escin is plotted. (C) Excised tumor weights of (a) PC-3 and (b) DU-145 were measured at the end of this study.

A

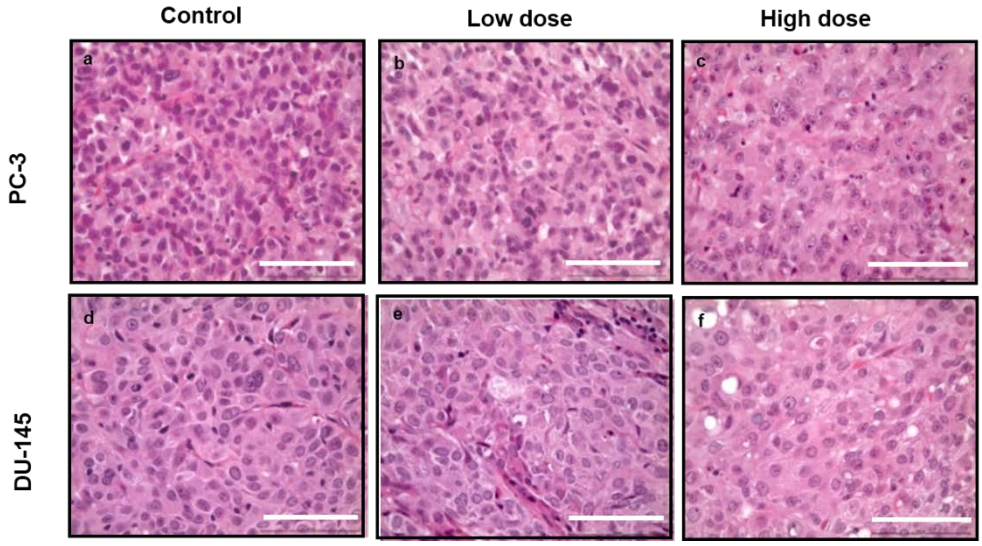

B

a

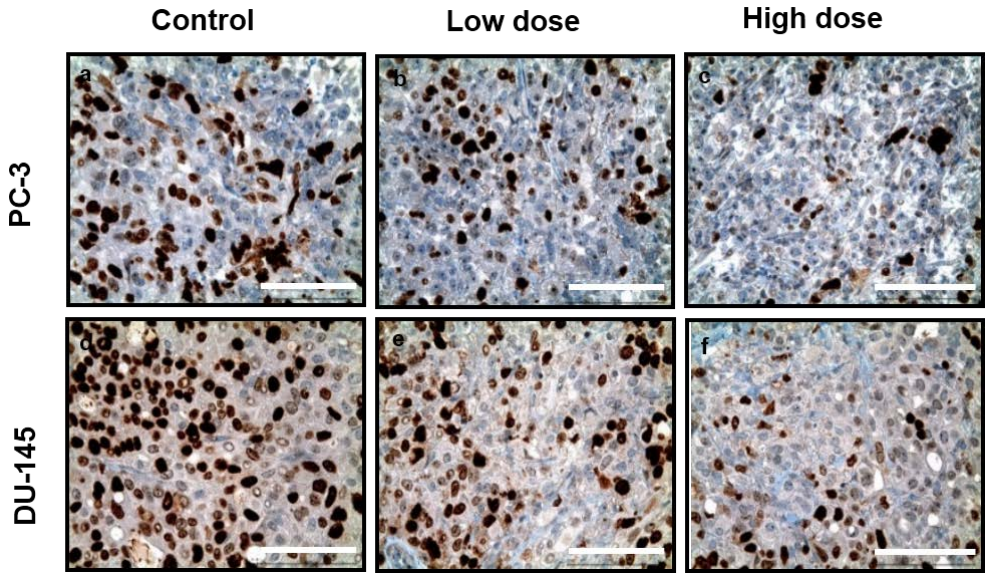
Control
Low dose
High dose
PC-3
DU-145
a
b
c
d
e
f

b

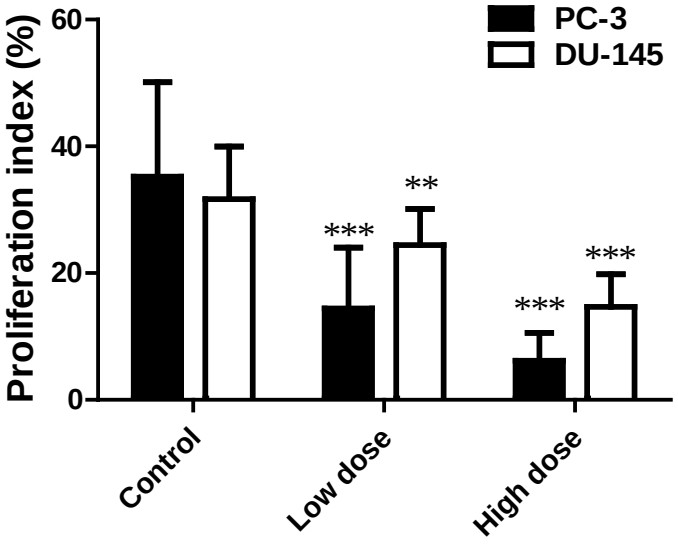
Proliferation index (%)
60
40
20
0
PC-3
DU-145
***
**
***
***
Control
Low dose
High dose

B

a

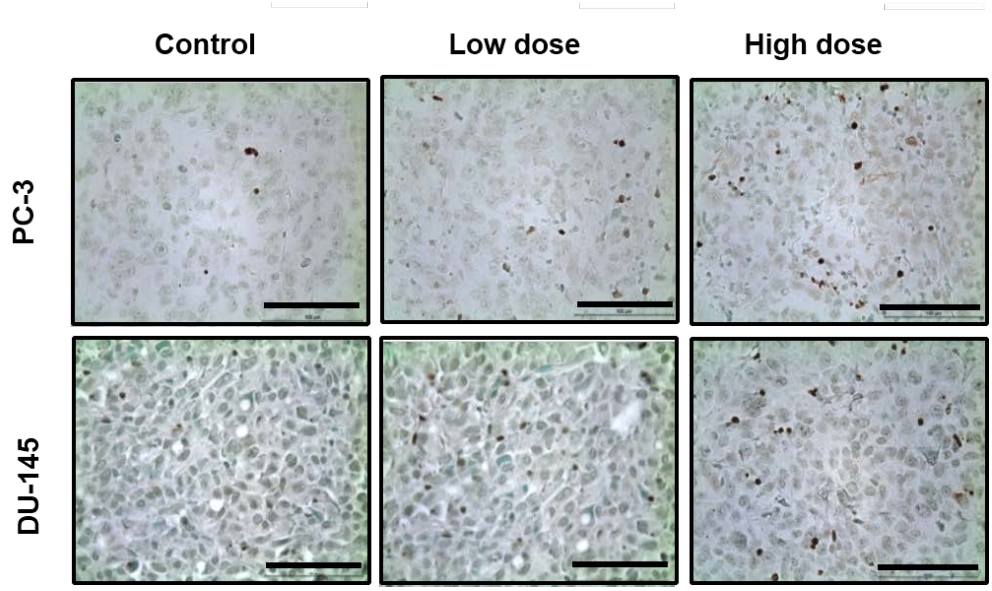
Control
Low dose
High dose
PC-3
DU-145

b

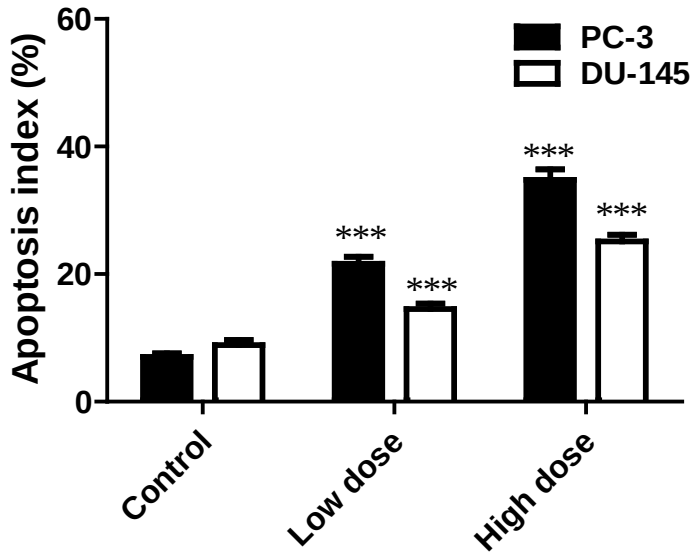
Apoptosis index (%)
60
40
20
0
PC-3
DU-145
***
***
***
***
Control
Low dose
High dose

Figure 11. Histologic and immunohistochemistric (IHC) analysis

(A) The H&E staining of tumor tissue. (B) (a) An analysis of the proliferation marker Ki-67 by an IHC analysis. (b) Ki-67-positive cells were counted to calculate the proliferation index. (C) (a) An analysis of tumor cell apoptosis based on a TUNEL assay. (b) TUNEL-positive cells were counted to calculate the apoptotic index. (A–C) Bar = 100 μm, magnification ×400. *, **, and *** indicate significance at the $p<0.05$, $p<0.01$, and $p<0.001$ levels, respectively.

Table 3. Effect of escin on tumor growth, body weight and organ index in CRPC xenograft models.

Group	Dose	IR (%)	Body weight (g)		Lung index	Heart index	Liver index	Kidney index	Spleen index
	(mg/kg) × d		Initial	Final	(mg/g)	(mg/g)	(mg/g)	(mg/g)	(mg/g)
PC-3									
Control	0	-	22.53±0.89	21.99±1.35	7.97±0.90	5.74±0.35	52.42±1.37	15.27±0.75	7.73±2.13
Low dose	1.4 × 21	33.53	22.42±0.70	22.21±0.76	8.64±0.95	5.23±0.59	48.06±3.99	18.48±1.09	8.07±1.07
High dose	2.8 × 21	46.07	23.19±1.38	22.10±1.36	8.54±0.73	4.75±0.49	47.95±4.50	18.10±1.94	7.83±0.76
DU-145									
Control	0	-	24.67±0.68	23.37±1.42	7.80±0.37	5.55±0.70	51.34±3.69	15.84±0.90	5.84±1.10
Low dose	1.4 × 21	13.86	24.24±2.03	23.63±1.47	8.11±0.86	5.52±0.63	50.66±2.23	15.86±1.12	6.39±1.27
High dose	2.8 × 21	28.87	25.33±0.91	23.89±1.77	8.23±1.00	5.85±1.33	53.71±5.89	16.76±0.57	6.30±1.77

Discussion

Although there are emerging evidences that escin has anti-tumor properties in various cancer cells, the effects of escin on human CRPC cells remain elusive. This study is the first to demonstrate the cytotoxic effect of escin on CRPC through the induction of apoptotic cell death and G2/M arrest. These results are consistent with those of previous studies. The effect of escin on CRPC cells may be attributed to the induction of apoptosis as well as the inhibition of the cell cycle checkpoints, which are common molecular mechanisms of anti-cancer agents (Gottesman 2002).

When there is apoptosis, many proteins modulate apoptotic signaling, including IAPs and Bcl-2 (Burz, Berindan-Neagoe et al. 2009). Among IAPs, cIAP-1 and cIAP-2 play key roles in the regulation of death-receptor-mediated apoptosis, whereas the X-linked IAP (XIAP) inhibits death-receptor- as well as mitochondria-mediated apoptosis by inhibiting caspase-3/-7 and caspase-9, key regulators for apoptosis (Chai, Shiozaki et al. 2001). These IAPs are strongly expressed in human cancer cells, whereas they are rarely so in normal cells (Salvesen and Duckett 2002). Bcl-2 proteins, including pro-apoptosis (Bax) and anti-apoptosis (Bcl-2 and Bcl-xL) proteins, are the most important regulators of the mitochondrial apoptosis pathway (Martinou and Youle 2011), and the ratio of Bax/Bcl-2 and Bax/Bcl-xL play an important role in the induction of apoptosis. Zhang *et al.* reported that escin-induced apoptosis was associated with both intrinsic (mitochondrial-mediated) and extrinsic (death-receptor-mediated) pathways in human acute leukemia cells (Zhang, Gao et al. 2011).

Other studies also revealed that escin-induced apoptosis was characterized by the decreased expression of antiapoptotic factors such as Bcl-2, Bcl-xL, and cIAP-2 (Harikumar, Sung et al. 2010, Ming, Hu et al. 2010, Tan, Li et al. 2010, Shen, Kang et al. 2011, Wang, Wang et al. 2012), and by a decreased the ratio of Bcl-2 to Bax (Shen, Kang et al. 2011, Zhang, Gao et al. 2011). Consistent with these findings, our results showed that escin suppressed the expression of BcL-2, BcL-xL, cIAP-1, cIAP-2, and xIAP while enhancing that of Bax.

Another distinct feature of apoptosis is the proteolytic cleavage of PARP by one or more caspases involved in the mitochondrial pathway, such as caspase-3. In the present study, the amount of total PARP decreased after treatment with escin in a time-dependent manner, whereas that of c-PARP increased, indicating escin induces apoptosis through both intrinsic and extrinsic signaling pathways in CRPC cells.

Interestingly, 24 μM of escin had a significant effect on G2/M arrest in PC-3 cells, whereas it had no such effect in DU-145 cells. Instead, a high dose of escin (44 μM) had a significant effect on G2/M arrest in DU-145 cells. This suggests that the expression of oncogene/tumor suppressor genes may contribute in part to cell-type-specific response to escin treatment. The retinoblastoma (Rb) tumor suppressor gene product phosphorylated-Rb (pRb) serves as a downstream mediator of p21 (Schafer 1998) and plays a crucial role in cell cycle control. Patlolla et al. (Patlolla, Raju et al. 2006) report that pRb is inhibited by escin. Qiu et al. (Qiu, Schönthal et al. 1998) demonstrate that the loss of functional pRb leads to G2/M arrest following p21 induction in the human osteosarcoma cell line Saos-2 . PC-3 cells express a normal

Rb protein, whereas DU-145 cells have a mutated Rb gene showing a loss of 105 nucleotides and encoding a truncated protein (Bookstein, Shew et al. 1990). In particular, the expression levels of p21 and pRb and the status of Rb appear vital in the cell cycle distribution by escin in CRPC cells. Future research should verify this hypothesis.

During G2, A-type cyclins are degraded by ubiquitin-mediated proteolysis while B-type cyclins are actively synthesized and able to bind free CDK1. The cyclin B1/CDK1 complexes are essential for initiating mitosis (M) (Jackman and Pines 1996, Smits and Medema 2001) and can phosphorylate a broad spectrum of proteins involved in regulatory and structural processes required for mitosis such as nuclear envelope breakdown, chromosomal condensation, fragmentation of the Golgi apparatus, formation of the spindle and attachment of chromosomes to it (Malumbres and Barbacid 2005). The activity of cyclin B1/CDK1 complexes can be suppressed by binding to CDK inhibitors such as p21 (Figure 12) (Jackman and Pines 1996). Our results showed that escin reduced the expression of cyclin B1 and CDK1 while enhancing that of $p21^{Cip1/Waf1}$ in both PC-3 and DU-145 cells, implying that these proteins may be involved in G2/M cell cycle arrest. $p21^{Cip1/Waf1}$ has been shown to regulate cell cycle progression in both G1 and G2 phases through p53-dependent or p53-independent pathways (Niculescu, Chen et al. 1998). Consistent with the findings of previous research (Patlolla, Raju et al. 2006), neither DU-145 nor PC-3 cell lines expressed functional p53 (Fan, Kumaravel et al. 2004) in the present study , suggesting that p53 may not play an essential role in escin-induced apoptosis or

$p21^{Cip1/Waf1}$ expression in CRPC cells. Because the anti-tumor activity of many conventional chemotherapeutic agents is mediated by p53 (Brown and Wouters 1999), the p53-independent activation of $p21^{WAF1/CIP1}$ triggered by escin treatment can represent an alternative therapeutic approach for prostate cancer patients who fail to respond to conventional agents targeting p53 .

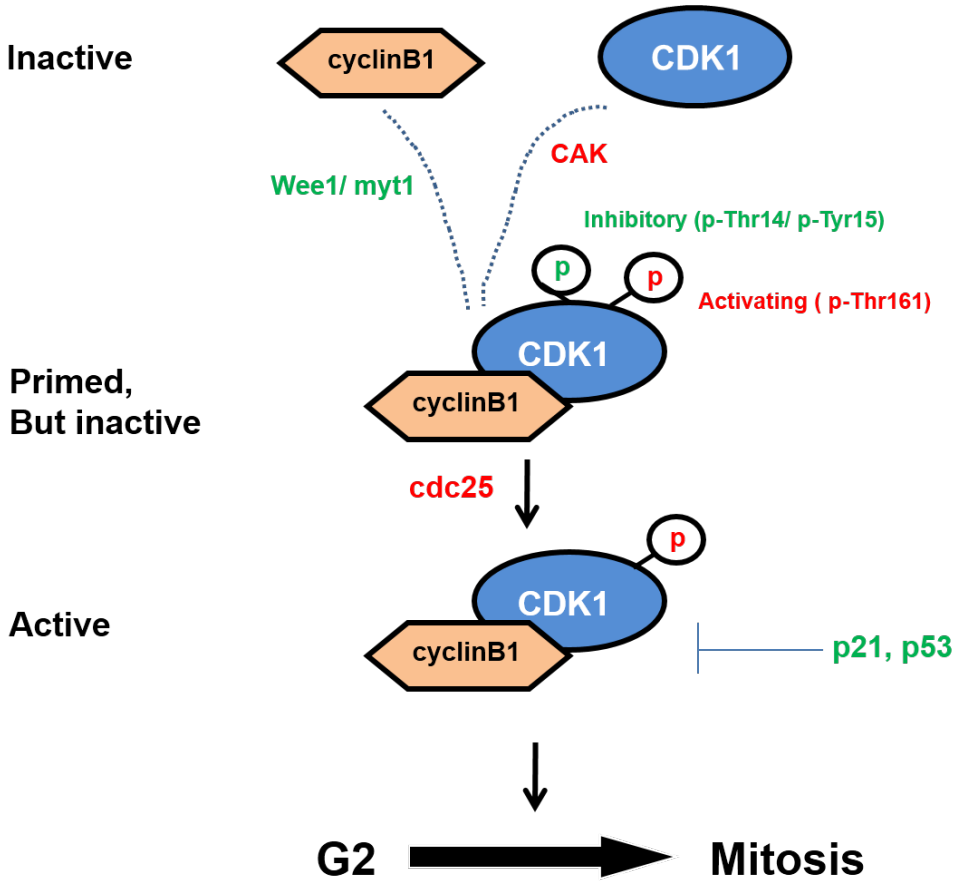

Figure 12. Phosphorylation events regulating CDK1 activity. Cyclin B is the regulatory subunit of CDK1. When CDK1 is not bound to cyclin B, it remains inactive. The CAK phosphorylates CDK1 at Thr161, ann event that is promoted by cyclin B binding to CDK1, and stimulates its activity. However, if CDK1 is also phosphorylated by Wee1/ Myt1 (on Thr14 and Tyr15), the kinase remains inactive. In late G2, the cdc25 dual specificity phosphatases activity and promoting entrance into mitosis (Stein and Pardee 2004).

Significant anti-tumor effects were still observed in escin treatment groups (see Figure 10). This study is the first to demonstrate, based on subcutaneous mouse models of CRPC, that escin may be effective in inhibiting tumor growth and that induction of apoptosis may be an important mechanism underlying the *in vivo* inhibition of tumor growth. Notably, escin-treated mice revealed no significant toxic effects, as evidenced by their maintained weight over the whole treatment period and the organ index in comparison to control groups at the end of the study. These results are expected to facilitate an in-depth analysis of the effects of escin on CRPC. Taken together, escin had cytotoxic effects on CRPC through the induction of apoptotic cell death and G2/M cell cycle arrest *in vitro* (Figure 13). And escin also suppressed tumor growth *in vivo*.

This study has some limitations. First, only one anti-tumor agent (escin) was used without any positive control of therapeutic agents to compare anti-tumor activity. Second, recent studies have reported that anti-tumor effects of chemotherapeutic agents are potentiated by escin in many human cancer cells, but the question of whether the same benefits can be realized for CRPC remains unanswered. In this regard, future research should test its efficacy in conjunction with other chemotherapeutic agents for CRPC. Third, apoptosis and cell cycle regulators were not analyzed *in vivo*. Here the question of whether escin induces changes in the levels of apoptosis and cell cycle regulators in cultured cells *in vivo* remains unanswered. Future research should address these issues to provide a better understanding of the anti-cancer effect of escin on human CRPC.

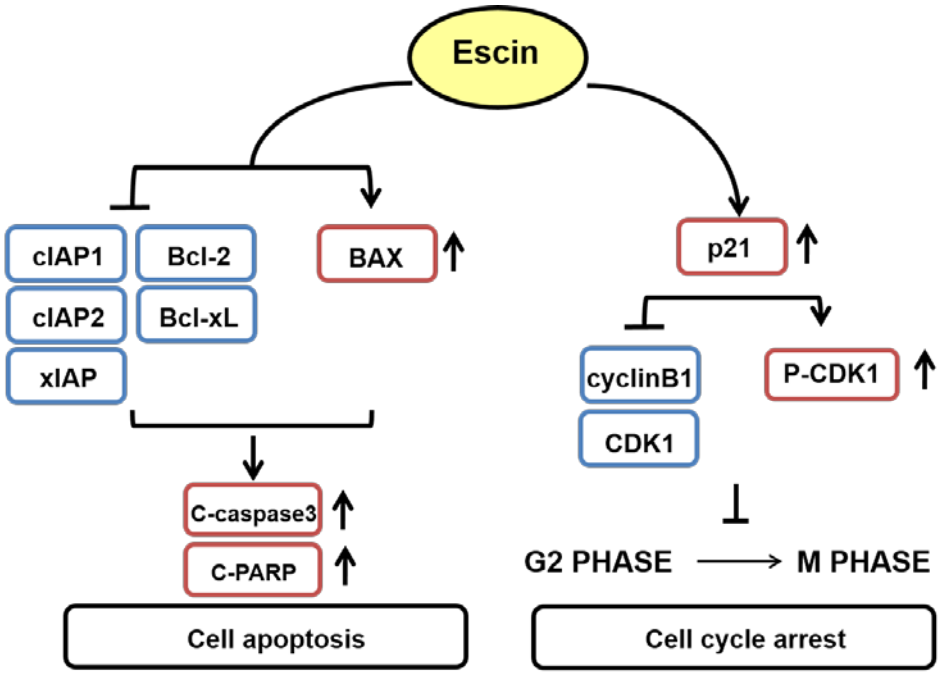

Figure 13. Schematic model of escin suppresses CRPC cells growth through the induction of apoptotic cell death and G2/M arrest.

Conclusion

The present study is the first to investigate both in vitro and in vivo antitumor effects of escin in human prostate cancer cells. The major findings including: 1) escin significantly inhibits prostate cancer cell growth; 2) escin induces cell apoptosis; 3) inhibition of cell proliferation and cell cycle progression appear to be major mechanism by which escin exerts its antitumor effects; 4) escin down-regulation of anti-apoptotic (cIAP-1, cIAP-2, XIAP, Bcl-2 and Bcl-xL) proteins, up-regulation of pro-apoptotic (Bax) protein; and 5) escin decreases the growth of CRPC xenograft tumors in mice, in a dose-dependent manner.

References

Baade, P. D., D. R. Youlden and L. J. Krnjacki (2009). "International epidemiology of prostate cancer: geographical distribution and secular trends." Molecular nutrition & food research **53**(2): 171-184.

Berridge, M. J. (2007). Cell signalling biology, Portland Press.

Bookstein, R., J.-Y. Shew, P.-L. Chen, P. Scully and W.-H. Lee (1990). "Suppression of tumorigenicity of human prostate carcinoma cells by replacing a mutated RB gene." Science **247**(4943): 712-715.

Brown, J. M. and B. G. Wouters (1999). "Apoptosis, p53, and tumor cell sensitivity to anticancer agents." Cancer research **59**(7): 1391-1399.

Burz, C., I. Berindan-Neagoe, O. Balacescu and A. Irimie (2009). "Apoptosis in cancer: key molecular signaling pathways and therapy targets." Acta oncologica **48**(6): 811-821.

Chai, J., E. Shiozaki, S. M. Srinivasula, Q. Wu, P. Dataa, E. S. Alnemri and Y. Shi (2001). "Structural basis of caspase-7 inhibition by XIAP." Cell **104**(5): 769-780.

Costantini, A. (1999). "Escin in pharmaceutical oral dosage forms: quantitative densitometric HPTLC determination." Il Farmaco **54**(11): 728-732.

D'amelio, M., V. Cavallucci and F. Cecconi (2009). "Neuronal caspase-3 signaling: not only cell death." Cell Death & Differentiation **17**(7): 1104-1114.

Fan, R., T. S. Kumaravel, F. Jalali, P. Marrano, J. A. Squire and R. G. Bristow (2004). "Defective DNA Strand Break Repair after DNA Damage in Prostate Cancer Cells Implications for Genetic Instability and Prostate Cancer Progression." Cancer research **64**(23): 8526-8533.

Fournier, P. (1948). Les plantes médicinales et vénéneuses de France, Paul Lechevalier.

Fu, F., Y. Hou, W. Jiang, R. Wang and K. Liu (2005). "Escin: inhibiting inflammation and promoting gastrointestinal transit to attenuate formation of postoperative adhesions." World journal of surgery **29**(12): 1614-1620.

Gottesman, M. M. (2002). "Mechanisms of cancer drug resistance." Annual review of medicine **53**(1): 615-627.

Hanahan, D. and R. A. Weinberg (2000). "The hallmarks of cancer." cell **100**(1): 57-70.

Harikumar, K. B., B. Sung, M. K. Pandey, S. Guha, S. Krishnan and B. B. Aggarwal (2010). "Escin, a pentacyclic triterpene, chemosensitizes human tumor cells through

inhibition of nuclear factor-κB signaling pathway." Molecular pharmacology **77**(5): 818-827.

Huerta, S., E. J. Goulet, S. Huerta-Yepez and E. H. Livingston (2007). "Screening and detection of apoptosis." Journal of surgical Research **139**(1): 143-156.

Jackman, M. and J. Pines (1996). "Cyclins and the G2/M transition." Cancer surveys **29**: 47-73.

Jeon, H. G., I. G. Jeong, J. Bae, J. W. Lee, J.-K. Won, J. H. Paik, H. H. Kim, S. E. Lee and E. Lee (2010). "Expression of Ki-67 and COX-2 in patients with upper urinary tract urothelial carcinoma." Urology **76**(2): 513. e517-513. e512.

Jung, K. W., Y. J. Won, H. J. Kong, C. M. Oh, D. H. Lee and J. S. Lee (2014). "Prediction of cancer incidence and mortality in Korea, 2014." Cancer Res Treat **46**(2): 124-130.

Kao, C., A. Martiniez, X. Shi, J. Yang, C. Evans, A. Dobi, R. Devere White and H. Kung (2014). "miR-30 as a tumor suppressor connects EGF/Src signal to ERG and EMT." Oncogene **33**(19): 2495-2503.

Kirby, M., C. Hirst and E. D. Crawford (2011). "Characterising the castration-resistant prostate cancer population: a systematic review." Int J Clin Pract **65**(11): 1180-1192.

Malumbres, M. and M. Barbacid (2005). "Mammalian cyclin-dependent kinases." Trends in biochemical sciences **30**(11): 630-641.

Malumbres, M. and M. Barbacid (2007). "Cell cycle kinases in cancer." Current opinion in genetics & development **17**(1): 60-65.

Martinou, J.-C. and R. J. Youle (2011). "Mitochondria in apoptosis: Bcl-2 family members and mitochondrial dynamics." Developmental cell **21**(1): 92-101.

Ming, Z., Y. Hu, Y. Qiu, L. Cao and X. Zhang (2010). "Synergistic effects of β-aescin and 5-fluorouracil in human hepatocellular carcinoma SMMC-7721 cells." Phytomedicine **17**(8): 575-580.

Nadiminty, N., R. Tummala, W. Lou, Y. Zhu, J. Zhang, X. Chen, R. W. deVere White, H.-J. Kung, C. P. Evans and A. C. Gao (2012). "MicroRNA let-7c suppresses androgen receptor expression and activity via regulation of Myc expression in prostate cancer cells." Journal of Biological Chemistry **287**(2): 1527-1537.

Niculescu, A. B., X. Chen, M. Smeets, L. Hengst, C. Prives and S. I. Reed (1998). "Effects of p21Cip1/Waf1 at both the G1/S and the G2/M cell cycle transitions: pRb is a critical determinant in blocking DNA replication and in preventing endoreduplication." Molecular and cellular biology **18**(1): 629-643.

Norbury, C. and P. Nurse (1992). "Animal cell cycles and their control." Annual review of biochemistry **61**(1): 441-468.

O'Brien, M. A. and R. Kirby (2008). "Apoptosis: A review of pro-apoptotic and anti-apoptotic pathways and dysregulation in disease." Journal of Veterinary Emergency and Critical Care **18**(6): 572-585.

Patlolla, J. M., J. Raju, M. V. Swamy and C. V. Rao (2006). "β-Escin inhibits colonic aberrant crypt foci formation in rats and regulates the cell cycle growth by inducing p21waf1/cip1 in colon cancer cells." Molecular cancer therapeutics **5**(6): 1459-1466.

Pittler, M. H. and E. Ernst (2006). "Horse chestnut seed extract for chronic venous insufficiency." Cochrane Database Syst Rev **1**.

Qiu, X.-B., A. H. Schönthal and E. Cadenas (1998). "Anticancer Quinones Induce pRb-Preventable G< sub> 2</sub>/M Cell Cycle Arrest and Apoptosis." Free Radical Biology and Medicine **24**(5): 848-854.

Salvesen, G. S. and C. S. Duckett (2002). "IAP proteins: blocking the road to death's door." Nature Reviews Molecular Cell Biology **3**(6): 401-410.

Schafer, K. (1998). "The cell cycle: a review." Veterinary Pathology Online **35**(6): 461-478.

Shapiro, G. I. (2006). "Cyclin-dependent kinase pathways as targets for cancer treatment." Journal of Clinical Oncology **24**(11): 1770-1783.

Shen, D. Y., J. H. Kang, W. Song, W. Q. Zhang, W. G. Li, Y. Zhao and Q. X. Chen (2011). "Apoptosis of Human Cholangiocarcinoma Cell Lines induced by β-Escin through Mitochondrial Caspase-dependent Pathway." Phytotherapy Research **25**(10): 1519-1526.

Siegel, R., J. Ma, Z. Zou and A. Jemal (2014). "Cancer statistics, 2014." CA: a cancer journal for clinicians **64**(1): 9-29.

Smits, V. A. and R. H. Medema (2001). "Checking out the G< sub> 2</sub>/M transition." Biochimica et Biophysica Acta (BBA)-Gene Structure and Expression **1519**(1): 1-12.

Stein, G. S. and A. B. Pardee (2004). Cell cycle and growth control: Biomolecular regulation and cancer, John Wiley & Sons.

Tan, S. M.-L., F. Li, P. Rajendran, A. P. Kumar, K. M. Hui and G. Sethi (2010). "Identification of β-escin as a novel inhibitor of signal transducer and activator of transcription 3/Janus-activated kinase 2 signaling pathway that suppresses proliferation and induces apoptosis in human hepatocellular carcinoma cells." Journal of Pharmacology and Experimental Therapeutics **334**(1): 285-293.

Wang, Y.-W., S.-J. Wang, Y.-N. Zhou, S.-H. Pan and B. Sun (2012). "Escin augments the efficacy of gemcitabine through down-regulation of nuclear factor-κB and nuclear factor-κB-regulated gene products in pancreatic cancer both in vitro and in vivo." Journal of cancer research and clinical oncology **138**(5): 785-797.

Zhang, Z., J. Gao, X. Cai, Y. Zhao, Y. Wang, W. Lu, Z. Gu, S. Zhang and P. Cao (2011). "Escin sodium induces apoptosis of human acute leukemia Jurkat T cells." Phytotherapy Research **25**(12): 1747-1755.

Zhou, X. Y., F. H. Fu, Z. Li, Q. J. Dong, J. He and C. H. Wang (2009). "Escin, a natural mixture of triterpene saponins, exhibits antitumor activity against hepatocellular carcinoma." Planta Med **75**(15): 1580-1585.

국문 초록

전립선암은 최근 빠른 증가 추세를 보이는 남성 암으로써, 외과적 절제/ 방사선 치료에도 불구하고 15-30%에서는 호르몬 불응성 전립선암으로 진행하게 된다. 호르몬 불응성 전립선암으로 진행될 경우 항암화학요법이 시행되고 있지만 생존률 증가 효과가 낮아, 효과적인 치료제의 개발이 시급한 실정이다. 최근, 천연 추출물인 Escin이 다양한 악성 종양에서 항암 효과를 보인다는 점에 착안하여 escin이 호르몬 불응성 전립선암에서 항암 효과를 효과적으로 유발하는지에 대해 *in vitro* 및 *in vivo*에서 검증하고, 그 기전을 규명하는 것이 본 연구의 목적이다.

세포성장 억제 및 관련 기전을 알아보기 위해, 호르몬 불응성 전립선암 세포주에 Escin 을 다양한 농도와 시간으로 처리한 후, 세포의 생존률, 세포고사 유도 및 관련 단백질 발현 여부를 분자 수준에서 확인하였다. Escin 의 항암 효과가 실제 생체 수준에서도 나타나는지에 대한 검증을 위해 면역억제 마우스에 호르몬 불응성 전립선암 세포주를 피하이식한 후 Escin 을 처리한 후 종양의 성장 억제 여부를 관찰하였다.

호르몬 불응성 전립선암 세포주에 escin 처리한 경우, escin 의 농도 및 처리 시간에 비례하여 세포 생존율이 감소하였고, 이는 세포고사 증가에 의한 것임을 확인하였다. 세포고사 유발 관련 단백질인 Bax, cleaved-caspase3 및 cleaved-PARP 가 증가하였고, 세포고사 억제 관련 단백질인 XIAP, cIAP-1, cIAP-2, Bcl-2, and Bcl-xL 감소하였다. 또한, 세포의 증식에 중요한 세포주기 중 특히, G2/M-phase 의 억제가 유도됨을 확인하였고, 이러한 세포주기 억제는 G2/M-phase 조절 단백질인 cyclin B1 및 CDK1 의

감소 및 p-CDK1 및 p21 증가에 의한 결과임을 분자 수준에서 확인하였다. In vitro 결과와 마찬가지로, 면역억제마우스에서 확립한 인간 호르몬 불응성 전립선암 이식 모델에서도 escin 의 처리에 의해 종양의 성장이 저해되는 것을 확인하였으며, 이는 면역조직화학 검사를 통해 세포의 증식이 저해되고, 세포 고사가 증가함에 따른 결과임을 검증하였다.

Escin 은 호르몬 불응성 전립선암 세포에서 세포고사 및 G2/M 세포 주기의 저해를 통해 세포의 생존 및 증식을 억제할 수 있으며, 이는 escin 이 호르몬 불응성 전립선암의 새로운 대안적 치료제로서의 가능성을 제시할 수 있는 과학적 근거 자료가 될 것으로 기대한다.

.....

주요어: Escin; 호르몬불응성 전립선암; 세포고사; 세포주기 억제

학번: 2012-30777